B. TECH. PROJECT REPORT

On

Nanocomposite of PANI and Carbon Dot Derived from Potato for Dye Adsorption

BY

Abhishek Kamat

DISCIPLINE OF METALLURGICAL ENGINEERING AND MATERIALS SCIENCE

INDIAN INSTITUTE OF TECHNOLOGY INDORE

December 2019

Nanocomposite of PANI and Carbon Dot Derived from Potato for Dye Adsorption

A PROJECT REPORT

Submitted in partial fulfillment of the requirements for the award of the degrees

of

BACHELOR OF TECHNOLOGY

In

METALLURGICAL ENGINEERING AND MATERIALS SCIENCE

Submitted by:

Abhishek Kamat

Guided by:

Dr. Dhirendra Kumar Rai

DISCIPLINE OF METALLURGICAL ENGINEERING AND MATERIALS SCIENCE

INDIAN INSTITUTE OF TECHNOLOGY INDORE

December, 2019

CANDIDATE'S DECLARATION

I hereby declare that the project entitled **"Nanocomposite of PANI and Carbon Dot Derived from Potato for Dye Adsorption"** submitted in partial fulfillment for the award of the degree of Bachelor of Technology in Metallurgical Engineering and Materials Science completed under the supervision of **Dr. Dhirendra Kumar Rai,** Assistant Professor in Discipline of Metallurgical Engineering and Materials Science, IIT Indore is an authentic work.

Further, I declare that I have not submitted this work for the award of any other degree elsewhere.

Signature and name of the student with date

CERTIFICATE by BTP Guide

It is certified that the above statement made by the student is correct to the best of my knowledge.

Signature of BTP Guide(s) with dates and their designation

Preface

This report on **"Nanocomposite of PANI and Carbon Dot Derived from Potato for Dye Adsorption"** is prepared under the guidance of **Dr. Dhirendra Kumar Rai**, Assistant Professor in Discipline of Metallurgical Engineering and Materials Science, IIT Indore.

The preparation, characterization and dye removal experiments in the form of adsorption studies have been performed for Polyaniline – Carbon dot nanocomposite. Reaction kinetic models and adsorption isotherm models have also been investigated to understand the nature of the reaction.

Abhishek Kamat
B.Tech. IV Year
Discipline of Metallurgical Engineering and Materials Science
IIT Indore

Acknowledgements

The overall experience for the past few months has been transformative in nature for me as a person. Going through the development phase of such a project is quite exhilarating. When the boundaries of understanding are uncharted, that is when the mind of an individual is really put to work. The road to scientific endeavors is nothing short of astoundingly challenging, but equally rewarding. This path has been really challenging for me. The constant valuable feedback from Dr. Dhirendra Kumar Rai has been integral to this work. The way that he thinks of his lab members as second family is something really new and inspiring for me. I'd also like to thank friends and family for being closely knit even through the tough times. People from the lab have had a constructive role to play in the whole timespan of this project. Mr. Sarathkumar has been through the thick and thin of this project along with me and the other B.Tech. students he really deserves a huge round of applause for his unending stream of efforts that I was a witness of.

Without the support of these people this task could not have been successfully fulfilled. May God bless them and help them through the path of their lives.

Abhishek Kamat
B.Tech. IV Year
Discipline of Metallurgical Engineering and Materials Science
IIT Indore

Abstract

Nanocomposite made of Carbon Quantum Dots (CDs) embedded in polymer (polyaniline) matrix has been prepared using a simple method, for dye removal application. Polyaniline has been prepared through a viable chemical oxidative polymerization, using APS (Ammoniumperoxysulfate) as the oxidizing agent in 1M H_2SO_4 reaction medium. CDs are prepared through a facile one-step hydrothermal method, using potato juice as a precursor, which gives a brown solution consisting of CDs dissolved in water. The prepared nanocomposite is environmentally benign, making it a viable replacement to other inorganic photocatalysts like TiO_2, ZnO and their derivatives.

The nanocomposite was characterized using Powder X-Ray Diffraction (PXRD), Fourier Transform Infra-Red (FTIR) Spectroscopy and Field Emission Scanning Electron Microscope (FESEM). A rod like morphology was observed in the nanocomposite. Characteristic XRD broad peaks at $2\boldsymbol{\theta} \approx 20$, 25 and 29^{o} have been observed, pointing out the successful preparation of the polymer PANI and that it possesses a highly amorphous nature. FTIR Spectra of the polymer and the nanocomposite corroborate the successful preparation of PANI. While a slight shift of peaks towards a lower wavenumber is observed in CD/PANI samples when compared to pure PANI. This is accounted for, by the bond modulation caused by the CDs in their neighboring region. All of the above results indicate successful preparation of the desired material, i.e. CD/PANI nanocomposite.

The materials were tested for use in dye removal through dye sdsorption route and CD/PANI performed much better in comparison to PANI. Though the adsorption capacities have only a slight difference, the rates of dye removal were drastically different. Two types of studies were administered: one where the contact time was varied and the other where the concentration of the original dye solution was varied. Both the materials show better coherence to the pseudo-second order kinetic model and the Freundlich adsorption isotherm. Methyl Orange dye was used for both types of dye removal experiments. Methyl Orange is a commonly used anionic dye that comes under the category of Azo dyes.

Table of Content

List of Figures

List of Tables

Chapter 1 Introduction

1.1 Prelude

In the modern era, the major problems that we face as a species are all, to some extent, by-product of our own actions since the start of the Industrial Age. A major chunk of these problems can be attributed to pollution of all different forms. Be it of air, water, land or any other kind. Some of these damages are considered irreparable. Meanwhile, vast amounts of research is being put into some of the ways that might help us tone down the amount of damage our actions cause to the environment.

A small chunk of the problems can also be attributed to the left over dyes and other industrial wastewater that are disposed into the environment and pollute our freshwater resource[3,4]. Currently, wastewater treatment activities are predominated by the use of inorganic oxides formulated into chemical and bio treatments[5]. For this purpose, different methodologies; like oxidation, reduction, photocatalytic degradation, adsorption and electrochemical reactions, are proposed to remove such contaminants from aqueous solutions[6]. Among these methods, dye adsorption is a leading solution that many opt for, towards the purpose of dye removal. What makes the use of adsorbents lucrative is the low cost – high abundance factor. Carbonaceous materials in the form of charcoals are the best example of generally used dye adsorbents[7]. Charcoal derived from various sources has been put to adsorption studies of various dyes in the recent years. Polymers and their composite derivatives also form a big part of the whole dye adsorption materials spectrum[8].

The prepared nanocomposite material and the pure polymer were prepared and tested under the same conditions. The characterization results point towards the successful preparation of the desired material. While the test results point towards a big leap in terms of adsorptive properties.

1.2 Background of Present Research

Carbon Quantum Dots(CDs) and Polyaniline(PANI) in their own right are novel materials and find their usage in a variety of applications ranging from: dye degradation in combination with other components like TiO_2, ZnO[9,10], supercapacitor electrode material[11,12] and heavy metal ion and organic molecule sensing[13,14,15], to name a few. CD on one hand, can be said to be the youngest member of the carbon nanomaterial family and were first obtained during purification of single-walled carbon nanotubes in 2004[16]. They demonstrate an array of desirable properties like high degree of functionalizability, low toxicity, and aqueous solubility[17,18]. PANI, the other crucial component of our desired nanocomposite, is a very important polymer in the class of conducting polymers, owing to its facile and good environmental stability, low cost preparation, non-toxicity, reversible electrochemistry and redox properties, etc[19]. It has a large variety of classical applications in sensors, secondary batteries, catalysis and electrostatic discharge protection[20,21,22].

The main goal of this study is preparing a nanocomposite constituting these two components in such a way that it enhances the properties of both the materials. Polymer-Carbon dot nanocomposite is being studied as of this day, for enhanced magnetism[23], visible spectrum absorption[10], photoluminescence[24], etc. PANI and its composites have been studied for adsorption properties before this as well[25, 26]. Table 1 is given below representing some such studies done in the past. The nanocomposite composed of polyaniline (PANI) with embeded carbon dots (CDs) hasn't been tested for dye removal properties to the best of my knowledge. And, promises a bright future in this field.

***Table 1**: Summary of adsorption capacities of PANI-based materials for dye removal.*

Material	Dye	Maximum adsorption capacity ($mg\ g^{-1}$)
PANI nanoparticle[27]	MB	6.2
PANI nanotube composite[28]	MB	9.1
PANI nanotube/silica[29]	MB	10.3
Nanostructured crosslinked PANI[30]	MB	13.8
PANI-HCl[31]	MO	75.9
PANI-CSA/polyamide 6 composite[32]	MO	81.9

(MB – Metylene Blue, MO - Methyl Orange.)

1.3 Objectives

A facile one-step route to CDs was adopted using potato juice as the precursor. Organic sources have been extensively researched towards the preparation of carbon quantum dots[9,24,33]. As for the preparation of PANI, chemical oxidative polymerization method was employed[34]. Elena et. al. proposed in their work that pH conditions during the polymerization process predominate over the morphology of polyaniline[34]. Using that valuable information, a consistent concentration i.e. 1M H_2SO_4 has been used in our experiment for all of the samples. Methods of synthesis adopted in this project require minimal inputs, making this method a viable contender for commercially viable production of the required nanocomposite.

Successfully characterizing the material is an important part of the whole research agenda. Techniques ranging from PXRD, FTIR spectroscopy, TGA and FE-SEM were used to comprehensively conclude the successful synthesis of the desired CD/PANI nanocomposite. The same characterizations have also been performed on

pure PANI samples. This gives the observer a comparative frame of reference towards the differences between these two products.

After successfully completing the prerequisite characterizations, comes time to put this novel nanocomposite to the test. Adsorption studies were carried out in 2 iterations, namely, contact time variation and concentration variation of the initial dye solution to understand the behavior of the material towards dyes. Methyl Orange, an anionic dye is used. The adsorption studies were performed for both the materials, i.e. PANI and CD/PANI. Using the results of these studies clear attributes can be associated to the incorporation carbon dots onto polyaniline matrix.

Chapter 2 Experimental

2.1. Preparation of Carbon Quantum Dots (CDs)

Preparation of CDs was carried out using the standard hydrothermal method, followed for the preparation of CDs from organic source, without the use of any special reagents[33]. To start with, potato juice was prepared in juice maker, without the addition of water. This juice was kept in the autoclave for 4hrs at a temperature of 120°C, followed by subsequent sonication for about 2hrs. The resulting suspension is filtered using normal filter paper. The filtrate is put into the Rota-evaporator. After this, as a final purification step, dialysis is performed. We get all the oversized particles and impurities out of the CD solution. This solution is then stored in the refrigerator. Later, it is used in the CD/PANI nanocomposite preparation without further purification.

2.2. Preparation of Pure Polyaniline

The polymer 2and the nanocomposites were prepared through oxidative polymerization route, wherein ammonium peroxydisulfate (APS) was used as the oxidizing agent. The reaction mixture had a composition of 0.25M APS, 0.2M Aniline. And 1M H_2SO_4 solution was used as the medium.

To start with, 1.094mL of aniline was dissolved in 20mL, 1M H2SO4. To this, 10mL, 1M H_2SO_4 solution is added drop wise, which consists of 2gm dissolved APS. The contents of this solution are then stirred for the next 30 min. A color change is observed in the solution, wherein it changes from white to black. The solution is stirred for the next 24 hours, during which the polymerization process occurs.

After the stirring is done with, the suspension is centrifuged to separate out the prepared polymer. A fine greenish-black powder gets sedimented at the bottom of the container. It was washed several times with water and ethanol, and with each wash its pH was checked. Washing was continued with water until the pH reaches a value of 6, subsequently, it was washed with a diluted solution of ethanol(10% ethanol, 90% water by volume) and the leftover particle slurry is put in the oven to dry overnight at a temperature of 70°C.

2.3. Preparation of CD/PANI Nanocomposite

The nanocomposite is prepared in a similar manner to the polymer. Just the addition of 2ml of as prepared CD solution is added to the mixture, before the addition of APS to the solution. This is to get CD firmly bonded to the PANI matrix. A flowchart is shown in figure 1, representing the procedure of preparation.

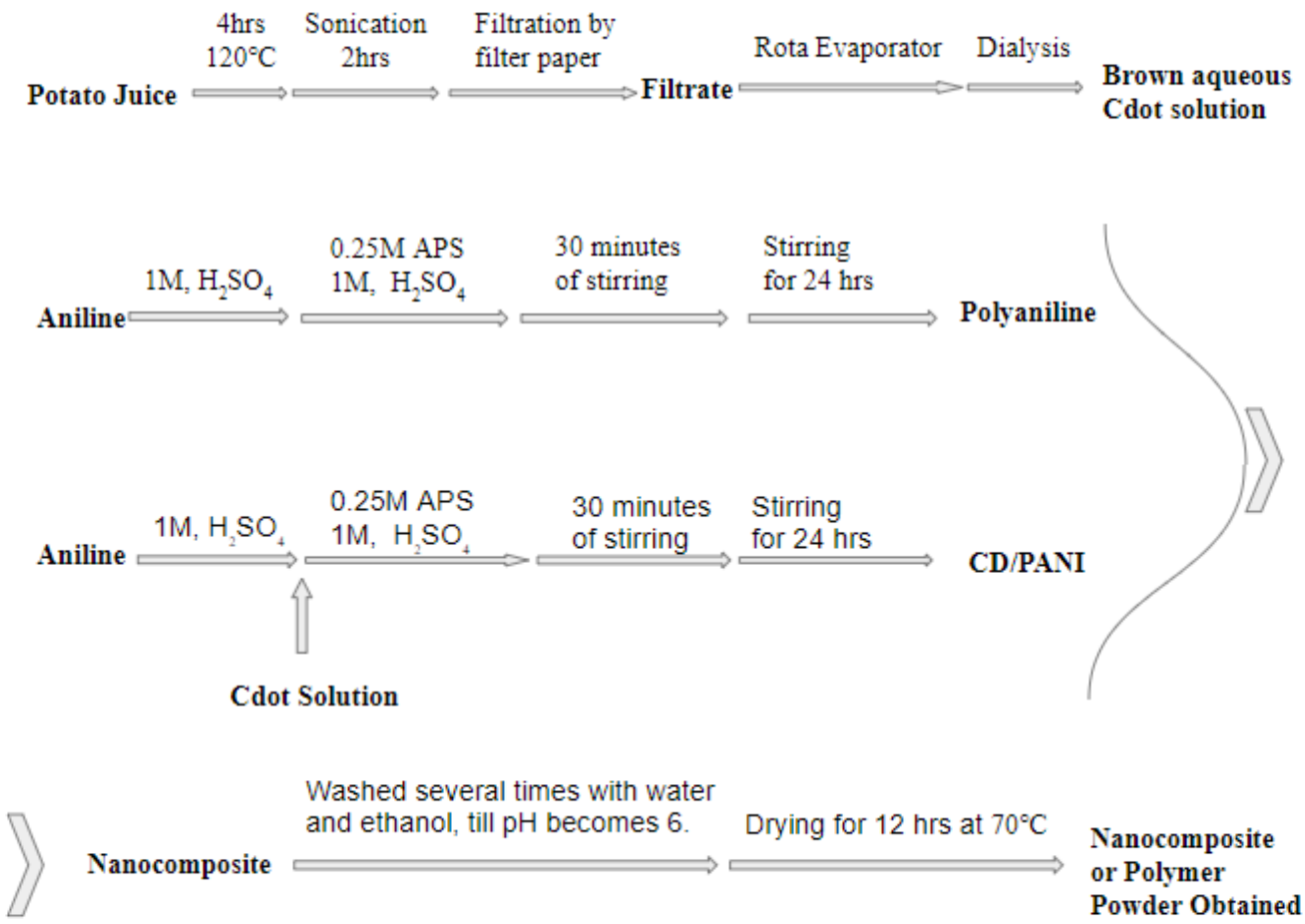

***Figure 1**: Flow chart representation of the preparation process.*

2.4. Dye Adsorption Studies

2.4.1. Effect of Contact Time on Dye Adsorption

The dye adsorption of methyl orange (MO) was carried out by adding 30 mg of photocatalyst in 70 mL of 50 mgL^{-1} MO solution at room temperature. The solution was stirred in the dark for 15 minutes using a magnetic stirrer. Later, the suspension was kept stationary in the dark for the next 3 hrs. A small amount of suspension (about 7 mL) was taken out every 30 min and centrifuged at 7000 rpm for 5 min to separate the adsorptive species from the degraded dye sample. The MO concentration in the leftover solution was quantified by the measurement of the decay of absorbance at $\lambda_{max} \approx 490$ nm.

2.4.2. Effect of Concentration on Dye Adsorption

Solutions of different concentrations (= 20, 40, 50, 60, 80 and 100 mg L^{-1}) were prepared using stock solution and 10 mL quantities were taken in separate vials, to every vial 10 mg of material was added. These solutions were stirred for 15 minutes and then they were put in the dark for a period of 3 hrs. During this period the vials were shaken from time to time. At the end of this time duration the suspensions were centrifuged at 7000 rpm for 5 min to remove the photocatalyst from the leftover solution. The MO concentration in the leftover solution was quantified by the measurement of the decay of absorbance at $\lambda_{max} \approx 490$ nm.

2.5. Characterizations

Powder X-Ray Diffraction (PXRD) in the range of $2\boldsymbol{\theta}$ = 10-50° was carried out using a Rigaku automated multipurpose X-ray diffractometer. Fourier Transform Infrared Radiation (FT-IR) transmission spectroscopy, was performed over a range of 400-4000cm^{-1}, using Perkin Elmer's Spectrum. Thermogravimetric Analysis (TGA) was performed on the temperature range of 30 - 900°C, on model TG209, NETZSCH. JEOL 7610 FPlus Field-emission Scanning Electron Microscope

(FESEM),at various magnifications were performed on the prepared samples. UV-Vis Spectrometer was used to check the intensities of the degraded dye samples.

Chapter 3 Results and Discussion

3.1. PXRD Analysis

The PXRD peaks of pure PANI and CD/PANI highly correspond with the experiments conducted by Liu et. al.[23] with characteristic peaks of pure PANI around $2\boldsymbol{\theta} \approx 20.3°$, 25.3° and 29.5° (Figure 2). PXRD plots of the polymer and its nanocomposite show no discernible features with regard to their peak positions. This can be attributed to the miniscule quantity of CDs present in the polymer matrix. These observed peaks can be attributed to the emeraldine salt (ES) phase of PANI. Broadness of XRD peaks is typical of polymers due to their amorphous nature. This is also true in the case of PANI as can be inferred from the presence of broad peaks in its XRD plot. The lattice planes of PANI associated with the intensity peaks' angles are mentioned in Table 1.

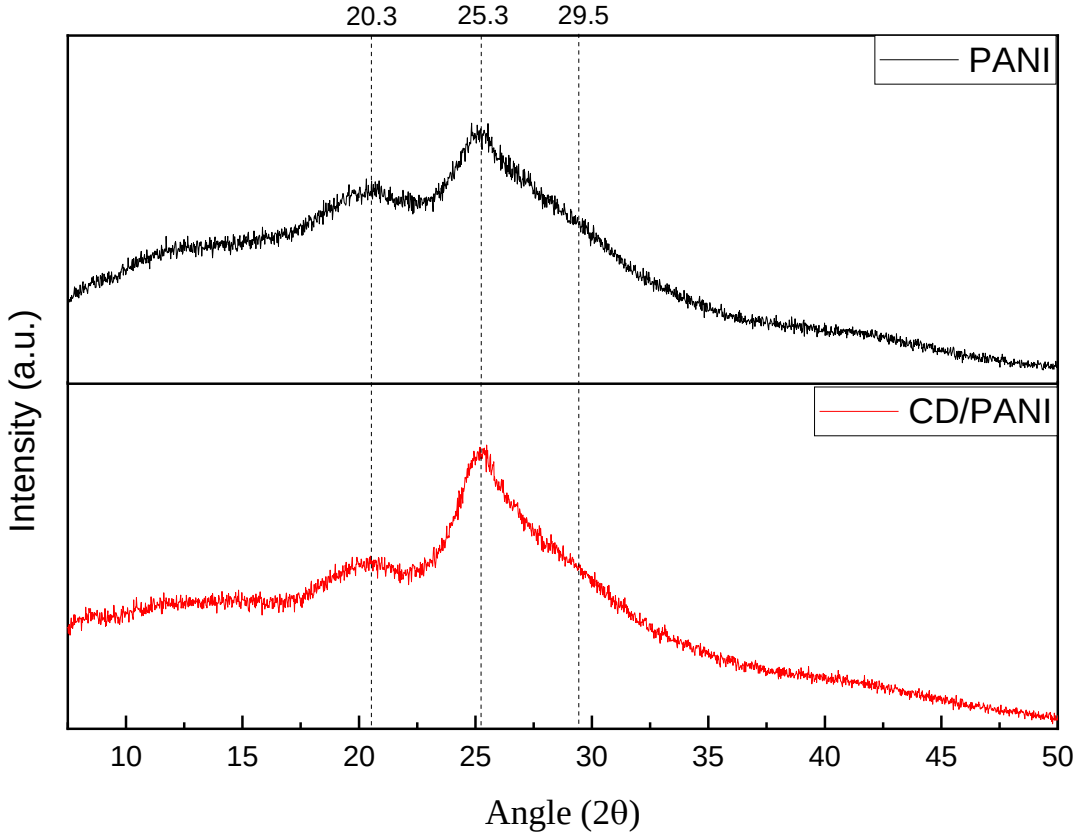

***Figure 2**: Powder X-ray diffraction (PXRD) plots of the prepared samples.*

***Table 2**: XRD peaks associated with PANI[7].*

S. No.	Angles of Peak Observation (2θ)	Angles (2θ) in ref. 7	Corresponding Crystallographic Plane of PANI
1.	*	9.1	(001)
2.	*	15.2	(011)
3.	20.3	20.3	(020)
4.	25.3	25.3	(200)
5.	*	27.4	(121)
6.	29.5	29.88	(022)

(* - peak not clearly discernible)

3.2. FTIR Analysis

The shift of peaks in the CD/PANI nanocomposite samples, when compared to the pure PANI sample has been observed as per the given plot (Fig. 3). This shift can be attributed to the CDs' presence in the polymer matrix. CDs tend to modulate the bond lengths of various species[2]. The peaks observed in the FTIR pattern of the prepared polymer correspond highly with the experimental findings of a study based on the same nanocomposite towards its application as supercapacitor electrode material[2]. Table 2 has been compiled referring to the same papers[1,2].

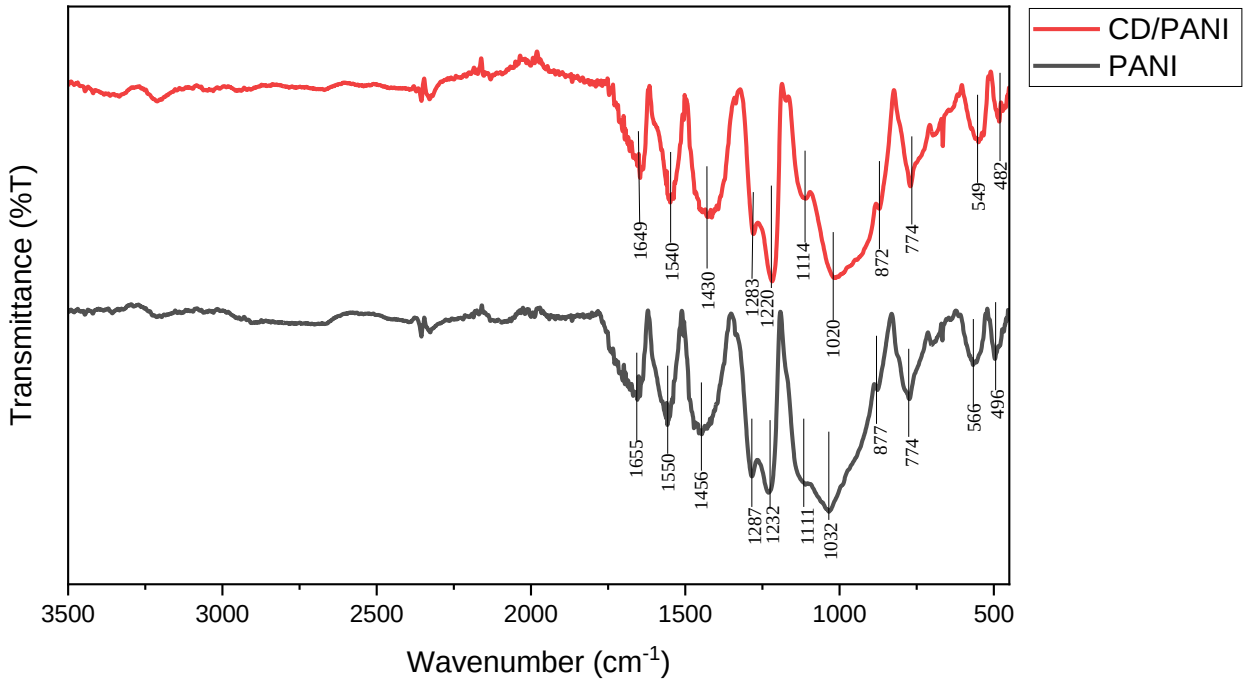

***Figure 3**: Fourier Transform Infrared-Radiation (FTIR) Spectra of PANI, CD/PANI.*

***Table 3**: FTIR peak assignment for PANI and its nanocomposite*[1,2].

No	Observed Peaks	Referred peaks	Assignment
1.	490-496 cm^{-1}	500 cm^{-1}	νC-H (Vibration mode)
2.	549-566 cm^{-1}	560 cm^{-1}	νCH_3-N
3.	770-774 cm^{-1}	769 cm^{-1}	Para-distributed aromatic rings
4.	872-877 cm^{-1}	878 cm^{-1}	γC-H (out-of plane deformation)
5.	1013-1034 cm^{-1}	1037 cm^{-1}	δC-H (in-plane deformation)
6.	1119 cm^{-1}	1111 cm^{-1}	(N=Q=N) (Q: quinoid ring)
7.	1218-1232 cm^{-1}	1240 cm^{-1}	νC-N
8.	1279-1287 cm^{-1}	1293 cm^{-1}	νC-N aromatic amines
9.	1421-1456 cm^{-1}	1480 cm^{-1}	νC=C (benzenoid ring)
10.	1538-1550 cm^{-1}	1550 cm^{-1}	νN-H, νC=C (quinoid ring)
11.	1645-1655 cm^{-1}	1650 cm^{-1}	νC=O

3.3. FESEM Analysis

Electron microscopy techniques have become a crucial part of modern day material analysis. SEM is one such technique and enables us in accomplishing high degrees of magnification and thus study the surface morphology of the material. The polymer PANI is known to assume a rod like and agglomerated morphology under general chemical oxidative polymerization processing. Under room temperature preparation, a rod like morphology with a low aspect ratio is acquired by the polymer (fig. 5 (c), (d)). The distinctly observable CD particles on the surface of nanocomposite, clearly indicate their successful attachment onto the polymer matrix (fig. 5 (c), (d)). The morphology of the nanocomposite highly corresponds to

the results observed by Zhao, Z. & Xie, Y. in their study towards electrochemical properties of the corresponding nanocomposite[11].

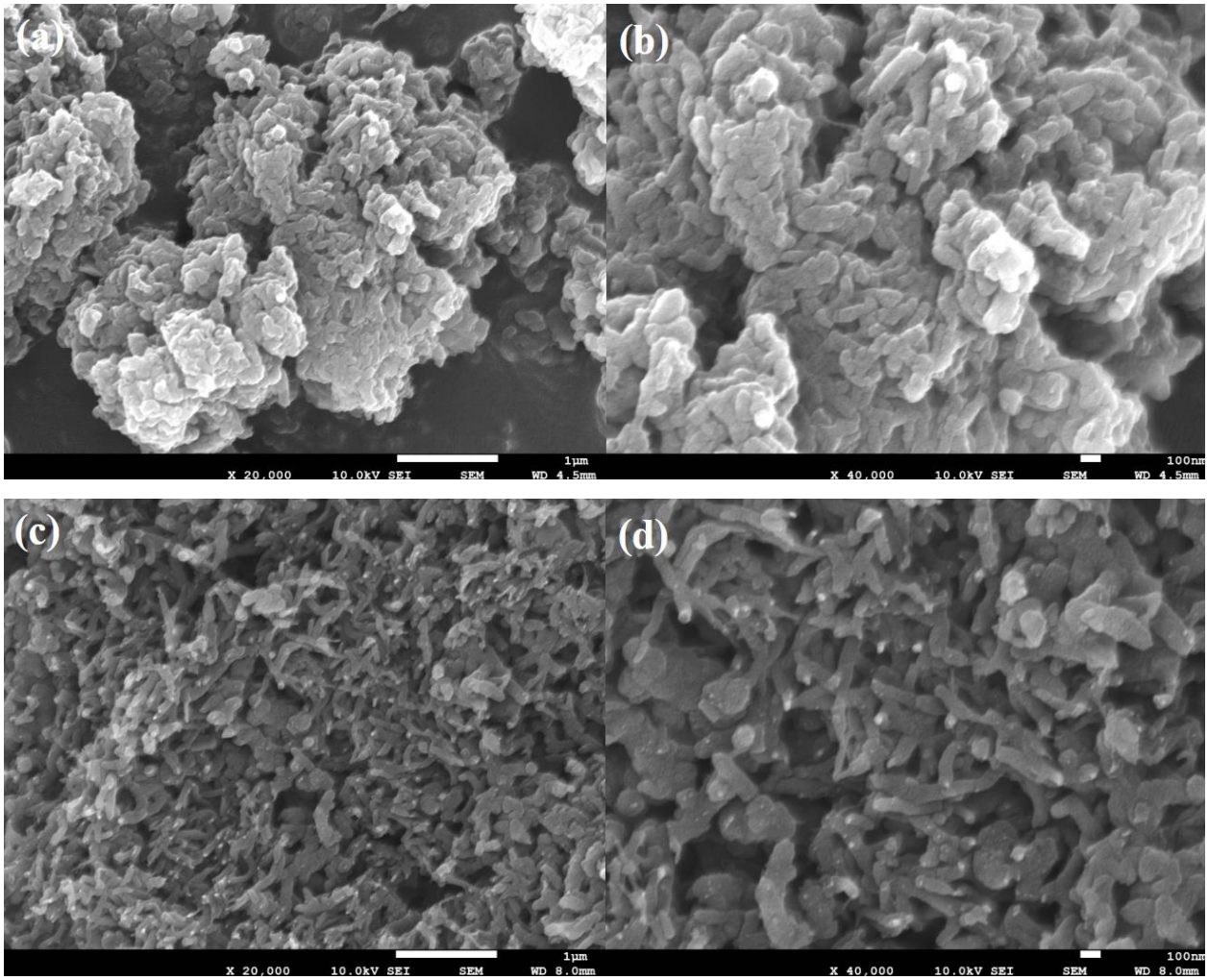

Figure 4*: FESEM Images of the pure PANI (a), (b) and CD/PANI (c), (d).*

3.4. Dye Adsorption Experiments

Using the peak values of intensities in the UV-Vis spectrometry of the degraded dye samples, their concentrations were quantified. A calibration curve was formed using standard solutions (of concentrations 20, 40, 50 and 60 mgL^{-1}), using which the concentrations of the resultant solutions were calculated. The formula mentioned below was used,

$$Equilibrium\ Concentration(Ce) = (Peak\ Intensity \times Slope\ of\ CL) - Intercept\ of\ CL$$

The concentrations thus calculated are used to find out the adsorption percentage with the help of this equation:

$$Adsorption\ (\%) = \frac{C_0 - C_e}{C_0} \times 100$$

Additionally, the equilibrium adsorption capacity of the material was quantified using,

$$q_e = \frac{V}{W} \times (C_0 - C_e)$$

Where, C_0 and C_e denote initial and equilibrium dye concentrations (mg L^{-1}), respectively. q_e stands for the equilibrium adsorption capacity of corresponding dye on the surface of adsorbent (mg g^{-1}), V is volume of dye solution in liters and W being weight of the adsorbent in grams.

3.4.1. Effect of Contact Time on Dye Adsorption

The plots represented in fig. 6 show the variation of concentration of MO dye in the samples collected at regular time intervals in comparison to the standard 50 mg L^{-1} solution which was initially taken. Later in this section the kinetics and adsorption isotherms are also discussed using the results of presented here.

a)

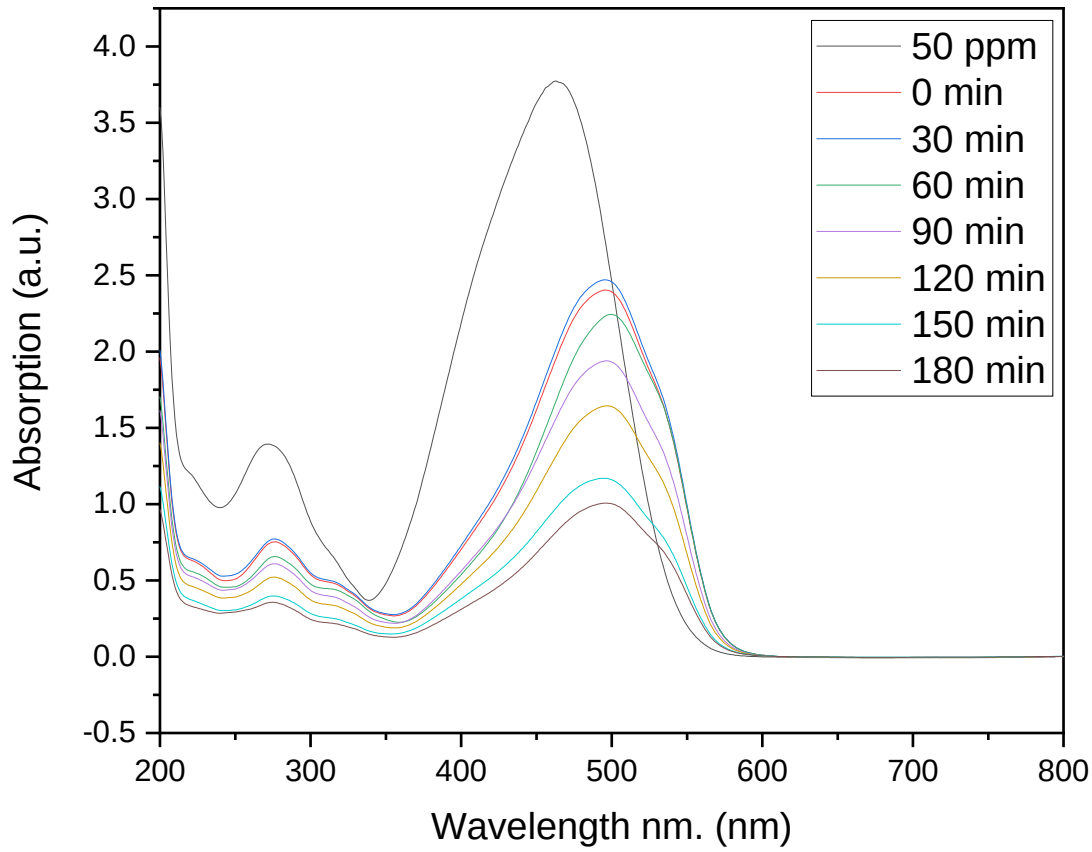
Absorption (a.u.)
Wavelength nm. (nm)
50 ppm
0 min
30 min
60 min
90 min
120 min
150 min
180 min
4.0
3.5
3.0
2.5
2.0
1.5
1.0
0.5
0.0
-0.5
200
300
400
500
600
700
800

b)

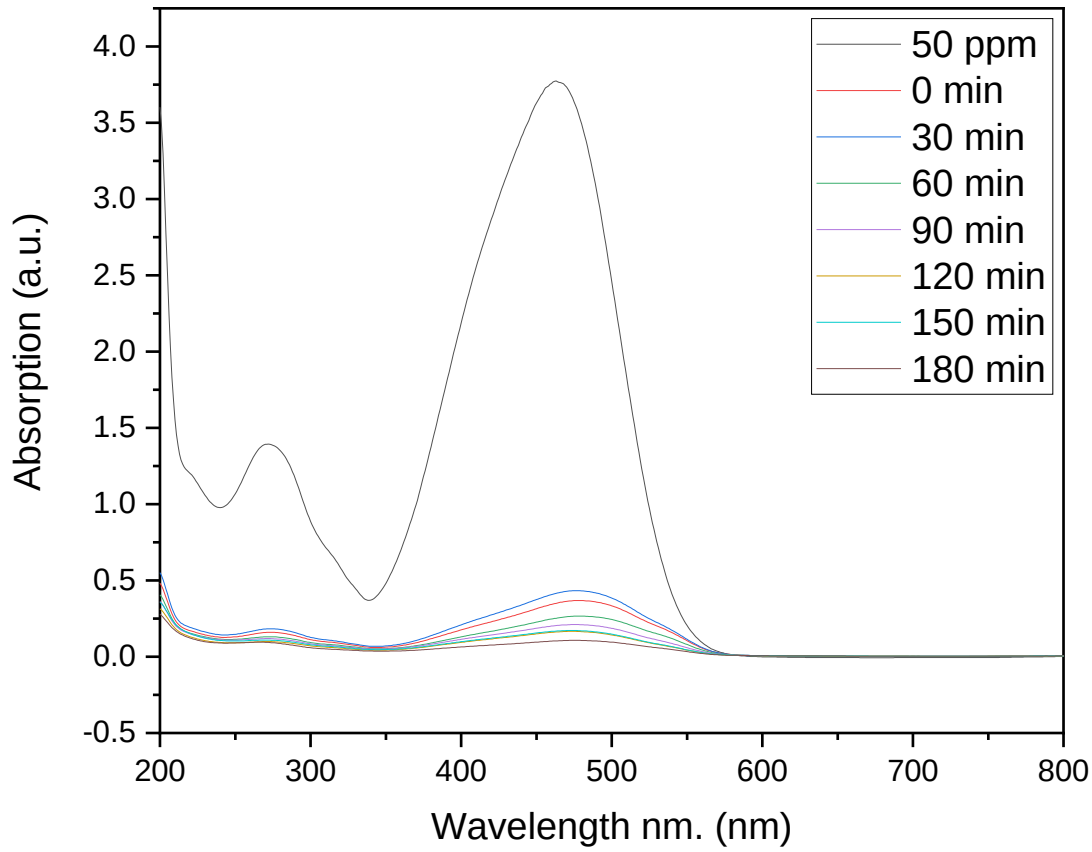

***Figure 5**: Adsorption of dye with respect to time. Using PANI (a) and CD/PANI (b).*

Here, a gradual loss in color over a period of 3 hrs was observed generally. The vast difference in the dye removal capability of PANI and CD/PANI are apparent from observing figure 7 and 8 respectively. The nanocomposite adsorbs the amount of dye in 15 minutes, which PANI takes more than 3 hrs to achieve. This fact alone makes the novel adsorption properties of CD/PANI obvious. The incorporation of CD's onto PANI has drastically improved its adsorption properties. Kinetics and isotherm studies predict the dye adsorption process to be following pseudo-second order and Freundlich isotherm models, respectively.

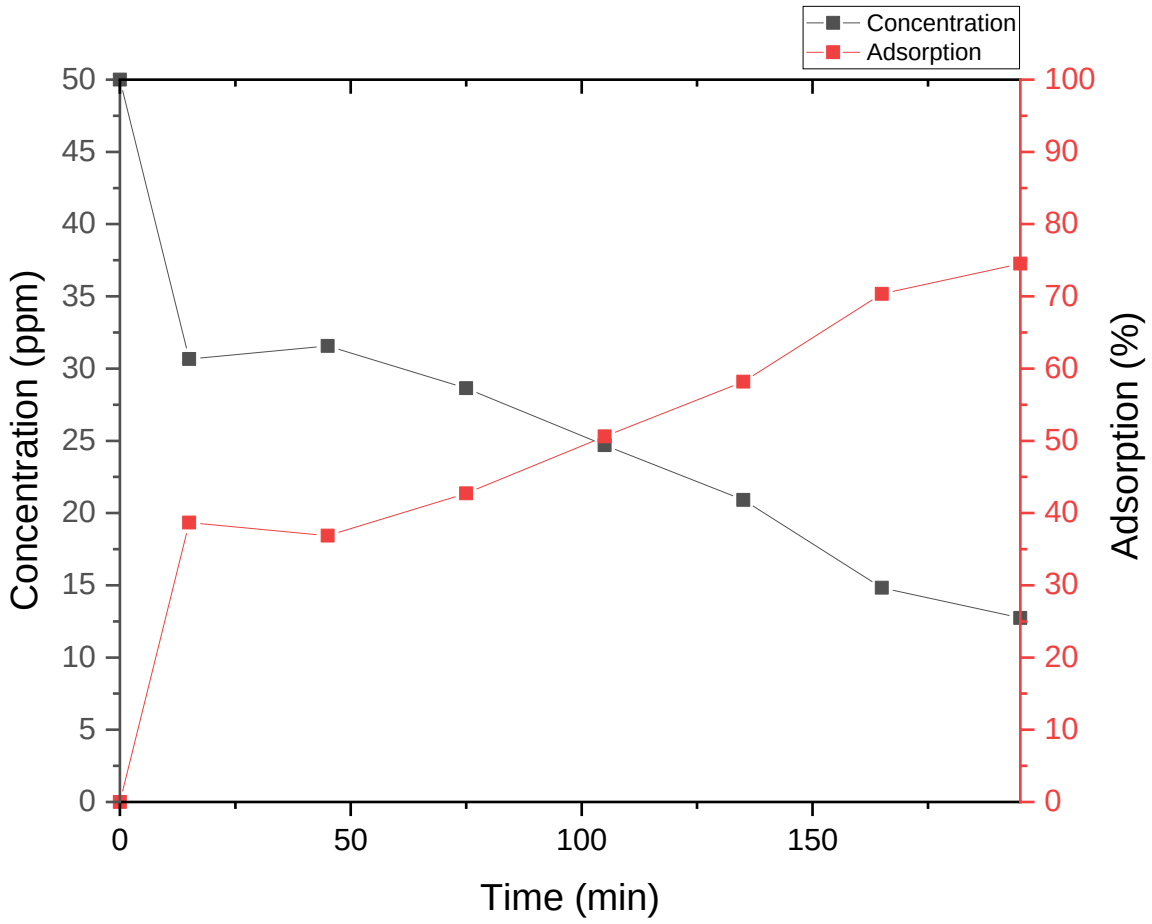

***Figure 6**: Time v/s concentration and adsorption % plot for PANI.*

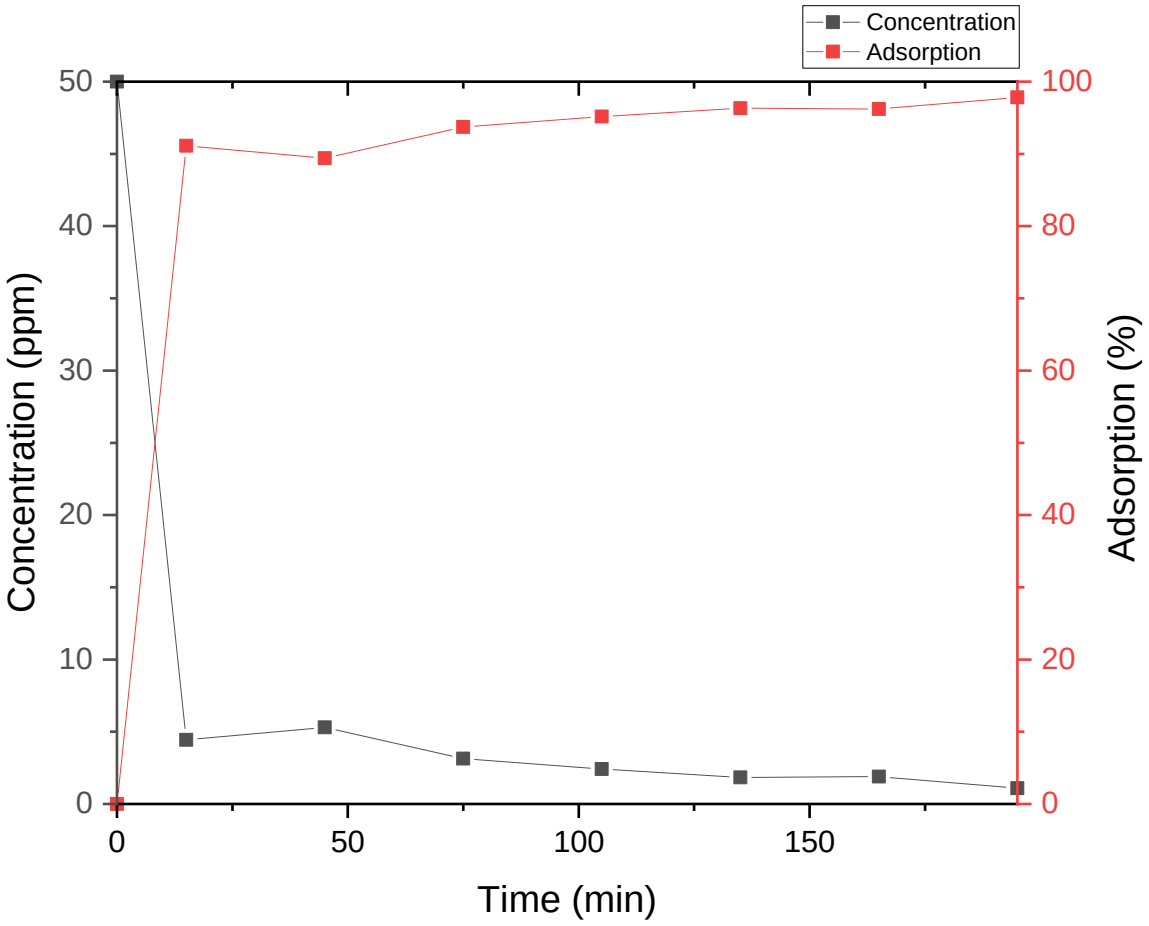

Figure 7: *Time v/s concentration and adsorption % plot for CD/PANI.*

3.4.2. Effect of Concentration on Dye Adsorption

Results of adsorption of MO dye samples of different concentrations using PANI and CD/PANI are represented in Figure 7. Here too, the concentrations of degraded samples are found using the calibration curve. The results homogeneously point towards the better adsorption qualities shown by CD/PANI, as the intensities of all the varied concentrated solutions after degradation were more for PANI as compared to CD/PANI.

A concentration dependent study helps us in determining the behavior of the adsorbent with respect to the dye concentration present in a particular solution. The ideal solution concentration to achieve high value of adsorption capacity can also be determined using this study. On the basis of these results, adsorption isotherm

studies have also been carried out, which point us towards Freundlich isotherm model being better suited for the prepared material.

a)

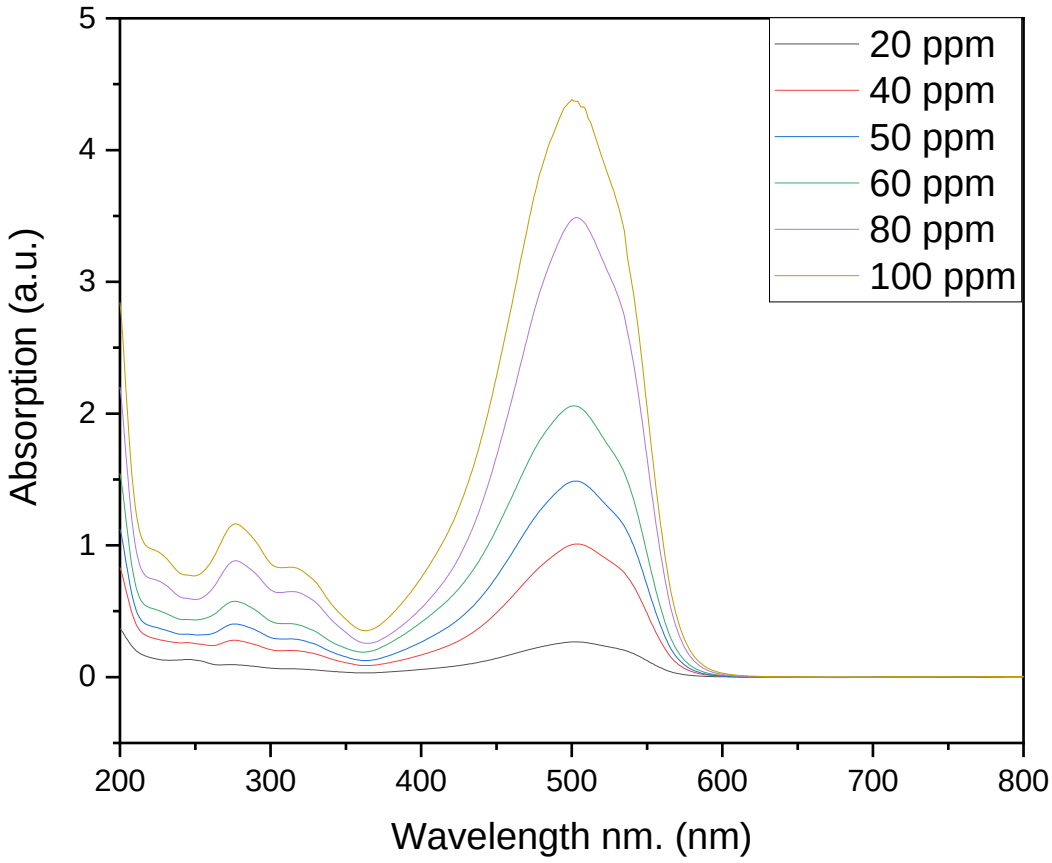

b)

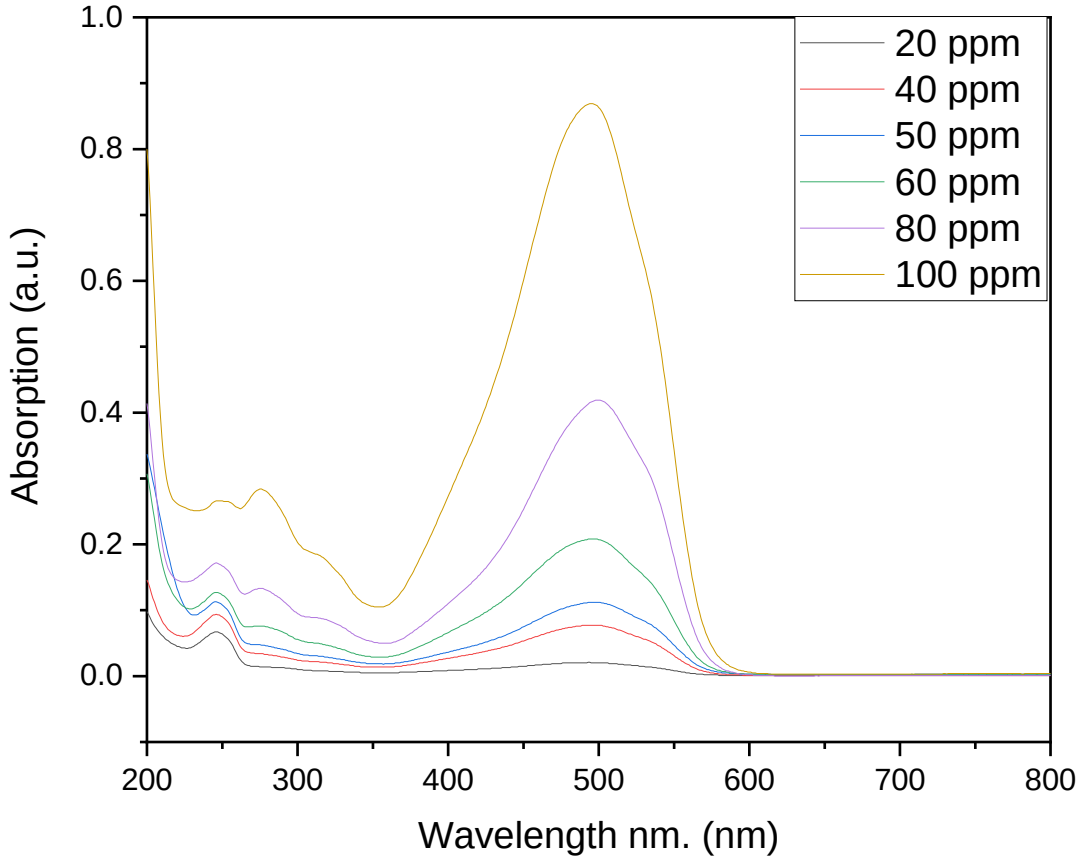

***Figure 8**: Degradation of dye with respect to concentration. Using PANI (a)and CD/PANI (b).*

3.4.3. Determining Order of the Reaction

The Legergren pseudo-first order[35] equation is represented as:

$$Log(q_e - q_t) = \text{Log}(q_e) - \frac{K_1}{2.303} \times t$$

Where, q_t and q_e (mg. g^{-1}) indicate the amount of dye that got adsorbed, per gram of adsorbent till a certain time (t) and equilibrium (end concentration) respectively and K_1 is the pseudo-first order rate constant. Figures 9 and 12 show the result of the linearly fitted plots of $Log(q_e - q_t)$ vs. t. The pseudo-first order reaction constants K_1, q_e and correlation coefficient (R^2) are collectively given in Table 3. The value of q_e needs to be separately calculated in the case of pseudo-first order kinetics

calculations. We get this value by curve fitting of the q_t v/s time plot (fig. 8, 11), and taking the stable value of q_t in the plot region to be q_e.

The pseudo-second order kinetic equation[35] is written in linear form as:

$$\frac{t}{q_t} = \frac{1}{K_2 \times q_e^2} + \frac{t}{q_e}$$

Here, K_2 (g mg $^{-1}$ min $^{-1}$) is the rate constant in the pseudo-second order equation. Figures 10, 13 show the plot of t/q_t vs. t for CD/PANI and PANI, respectively. Values of the parameters K_2, q_e and R^2 are listed in Table 3.

The curve between q_t and time (fig. 8, 11) is used to figure out the value of q_e (equilibrium adsorption), which needs to be known in order to figure out the pseudo first order rate constant K_1. Then a linear relation between log (q_e - q_t) and time (fig. 9, 12) is drawn out in correlation to the pseudo first order kinetics to get the value of K_1 using the value of slope received on curve fitting. Later on a linear relation is drawn between t/q_t and time (fig. 10, 13) according to pseudo-second order kinetics and the values of slope and intercept received in this relation are used to calculate q_e and K_2 (pseudo second order rate constant). All these derived values are used to make important inferences towards the reaction kinetics.

3.4.3.1. For CD/PANI:

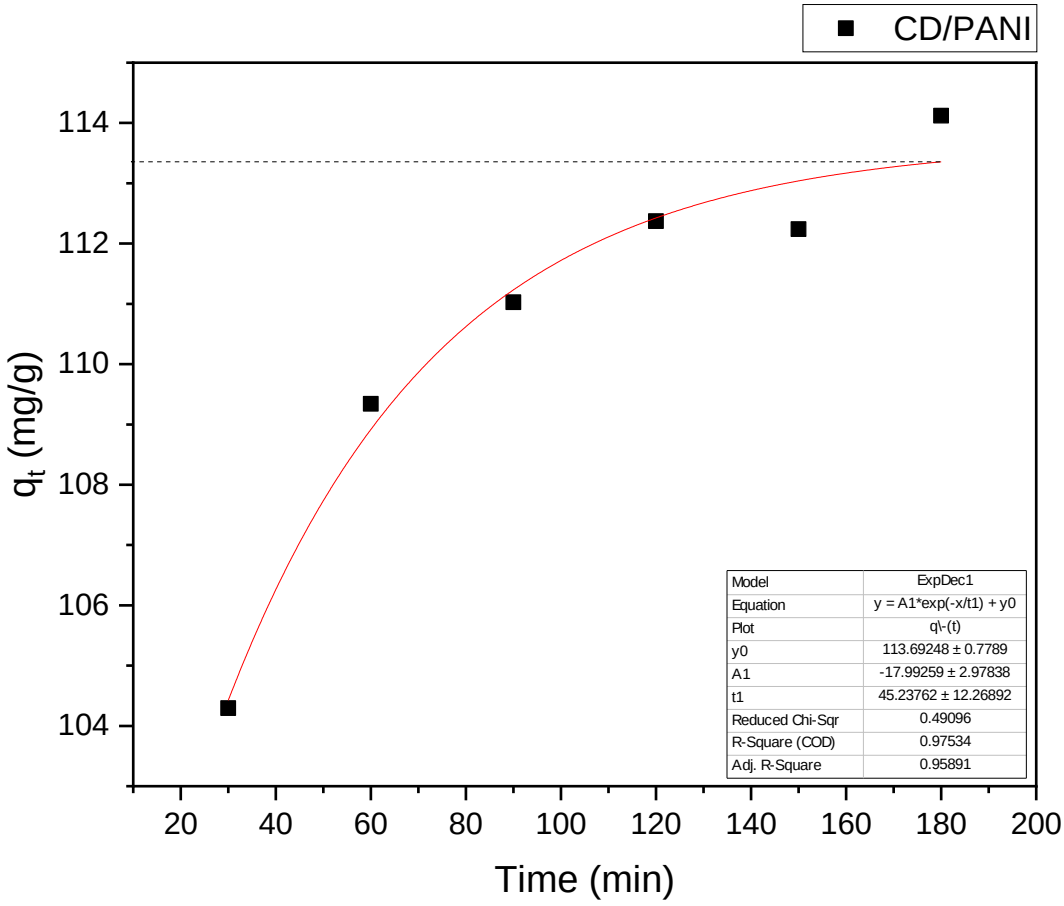

***Figure 9**: Determining valve of q_e using curve fitting for CD/PANI.*

Using this curve the q_e value was found out to be,

$$q_e = 113.22\, mg.g^{-1}$$

This value of q_e is used to get the values of log (q_e - q_t) at different time values. Which were then plotted in the form of figure 9.

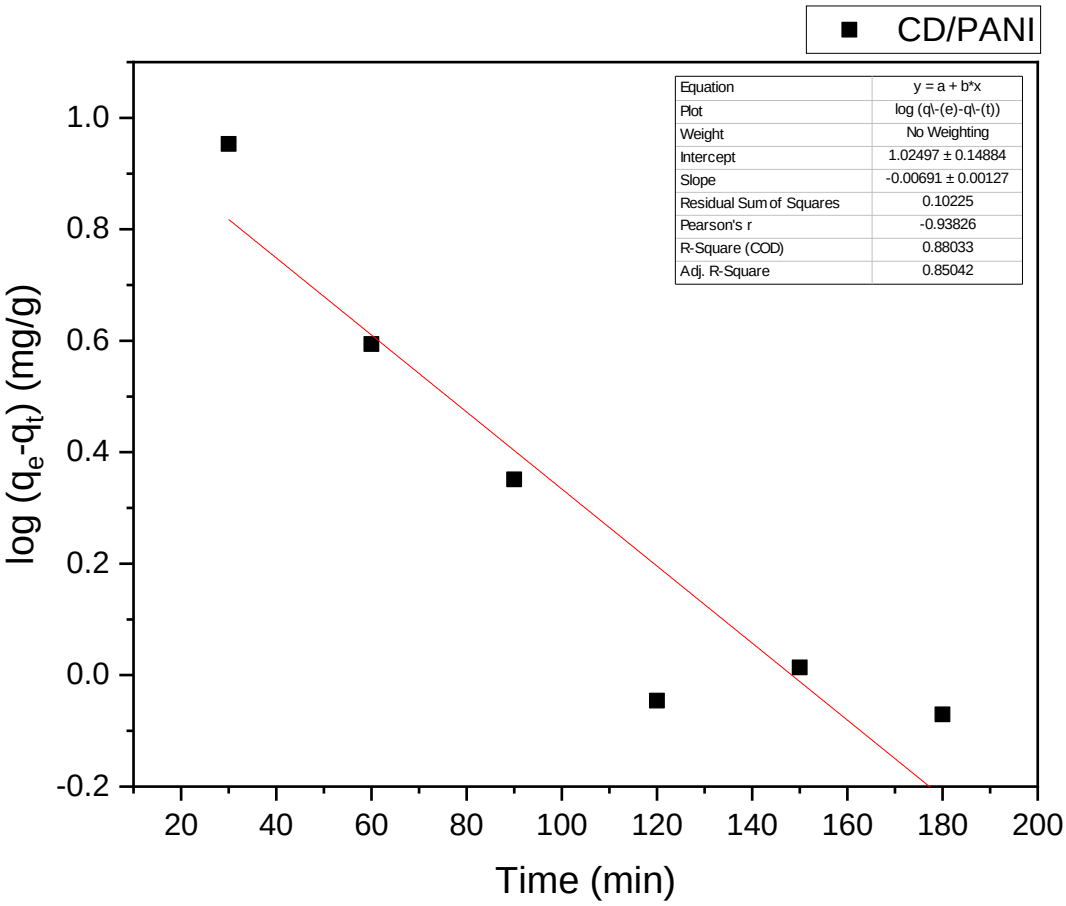

***Figure 10**: Pseudo 1st order reaction plot for CD/PANI.*

The information about the pseudo first order kinetics in mentioned below,

$$Slope = -0.00691$$

$$Intercept = 1.02497$$

Using the value of this line's slope K_1 is calculated using equation of pseudo first order rate kinetics as,

$$K_1 = -\big((-0.00691) \times 2.303\big) = 0.015914\ min^{-1}$$

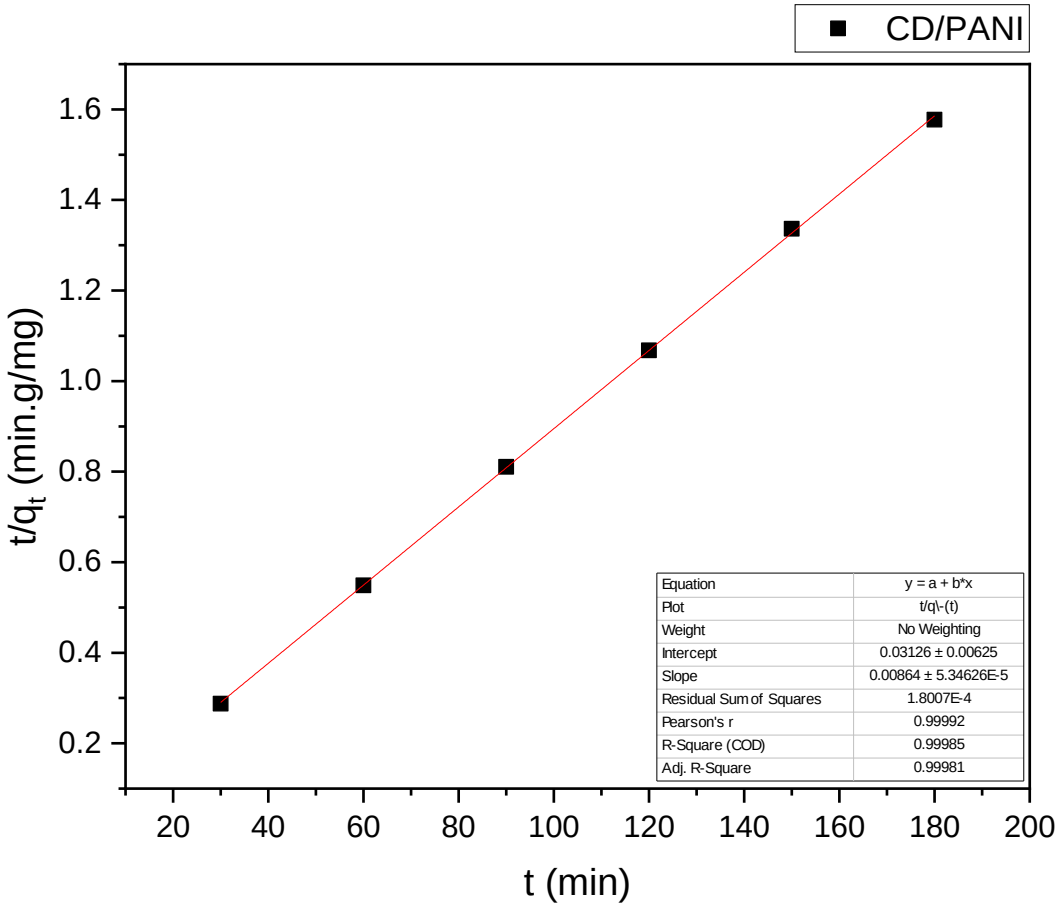

***Figure 11**: Pseudo 2nd order reaction plot for CD/PANI.*

The information about the pseudo second order kinetics in mentioned below,

$$Slope = 0.00864$$

$$Intercept = 0.03126$$

Using the value of this line's slope and its intercept, the values of q_e and K_2 are calculated using equation of pseudo second order rate kinetics.

$$q_e = \frac{1}{0.00864} = 115.74074\ mg.g^{-1}$$

$$K_2 = \frac{1}{(115.74074)^2 \times 0.03126} = 0.00241\ g.mg^{-1}min^{-1}$$

3.4.3.2. For PANI:

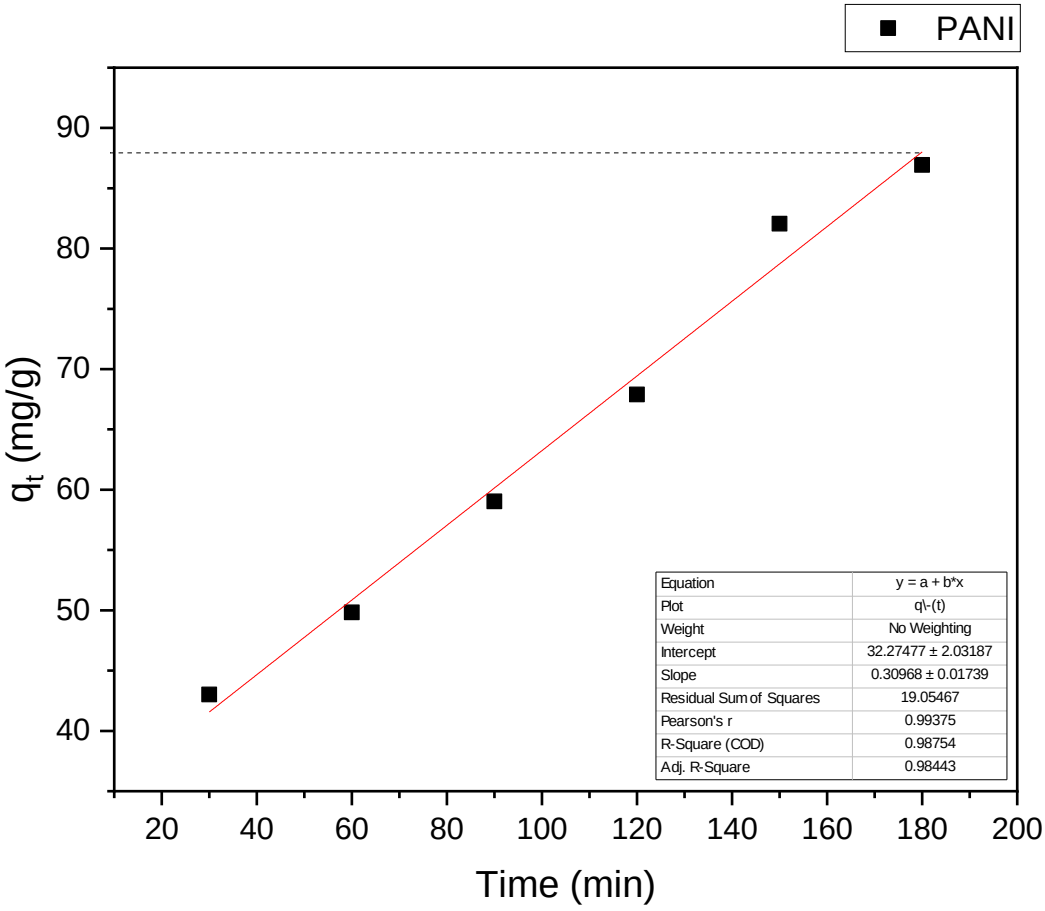

***Figure 12**: Determining valve of q_e using curve fitting for PANI.*

Using this curve the q_e value was found out to be,

$$q_e = 87.56\, mg.g^{-1}$$

This value of q_e is used to get the values of log (q_e - q_t) at different time values. Which were then plotted in the form of figure 12.

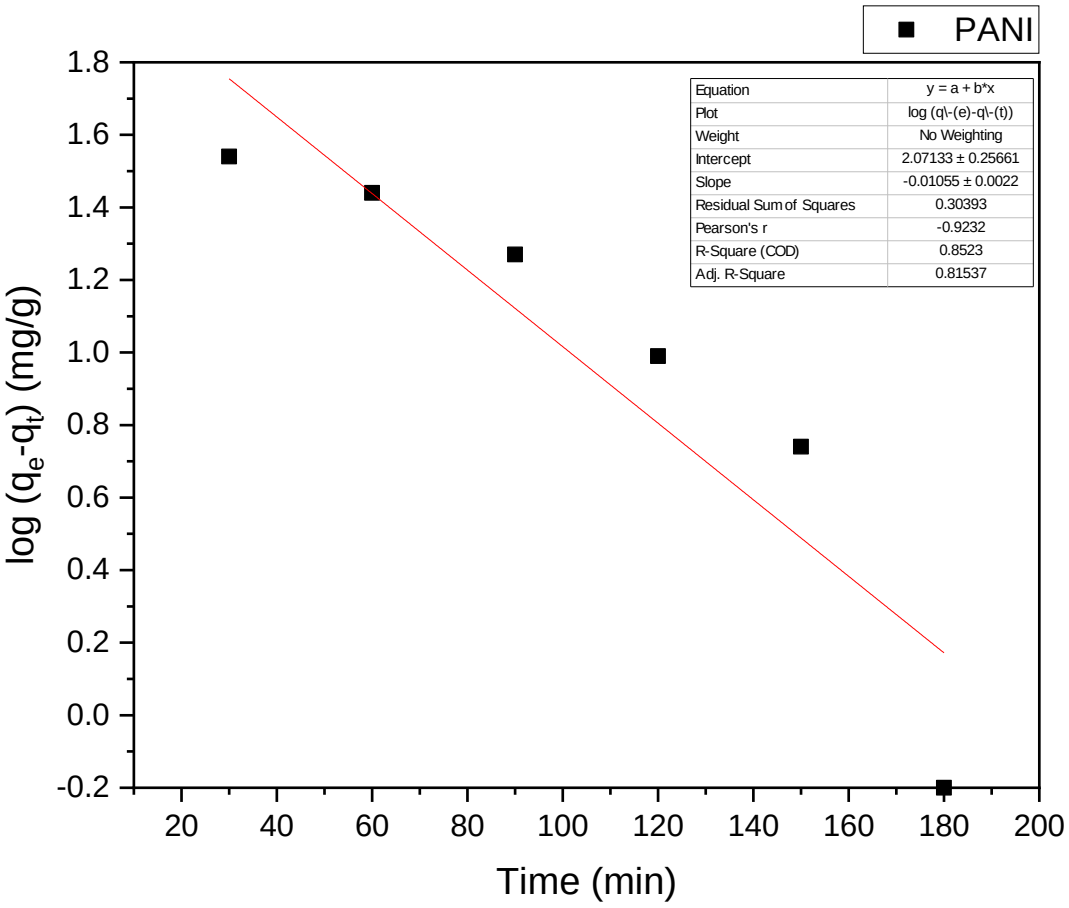

***Figure 13**: Pseudo 1st order reaction plot for PANI.*

The information about the pseudo first order kinetics in mentioned below,

$$Slope = -0.00102$$

$$Intercept = 2.20435$$

Using the value of this line's slope K_1 is calculated using equation of pseudo first order rate kinetics as,

$$K_1 = -\big((-0.01055) \times 2.303\big) = 0.02429\ min^{-1}$$

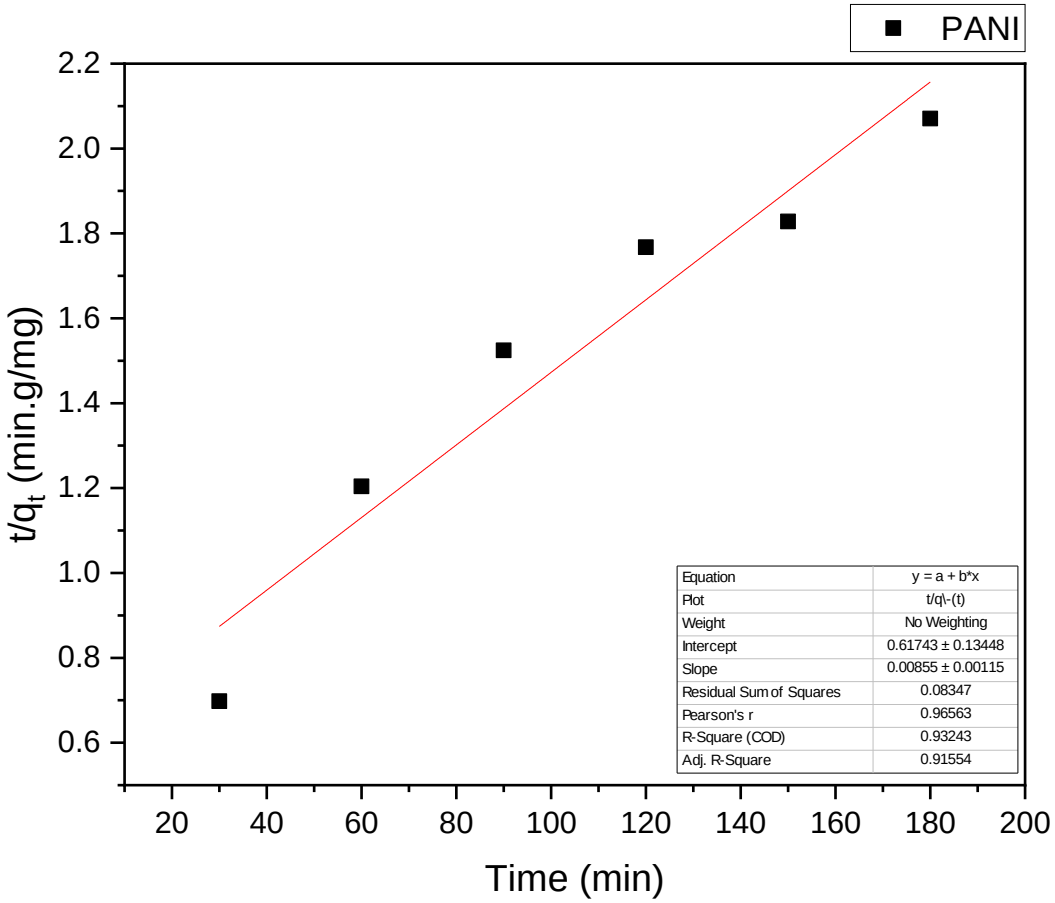

***Figure 14**: Pseudo 2nd order reaction plot for PANI.*

The information about the pseudo second order kinetics in mentioned below,

$$Slope = 0.00855$$

$$Intercept = 0.61743$$

Using the value of this line's slope and its intercept, the values of q_e and K_2 are calculated using equation of pseudo second order rate kinetics.

$$q_e = \frac{1}{0.00855} = 116.95906\ mg.g^{-1}$$

$$K_2 = \frac{1}{(116.95906)^2 \times 0.61743} = 0.00012\ g.mg^{-1}min^{-1}$$

***Table 4**: Values of constants associated with kinetics.*

S. No.	Adsorbents	Pseudo - First Order			Pseudo – Second Order		
		R^2	q_e ($mg.g^{-1}$)	K_1 (min^{-1})	R^2	q_e ($mg.g^{-1}$)	K_2 (min^{-1})
1.	CD/PANI	0.85042	113.22	0.01591	0.99981	115.74074	0.00241
2.	PANI	0.81534	87.56	0.02429	0.91554	116.95906	0.00012

Using these calculated values following observations are made and further information can be inferred. Firstly, higher values of R^2 (the correlation factor) for the for the pseudo-second order kinetics in case of both, PANI and CD/PANI are received. This indicates the nature of adsorption kinetics towards being second order. The adsorption capacities (q_e) are almost the same in value for both the adsorbents. The major difference lies in the values of rate constants (K_2) of the two adsorbents. As K_2 value of CD/PANI is more than 20 times that of PANI. Indicating that the rate of adsorption of the same dye being 20 times faster in the presence of CD/PANI than in the presence of same amount of PANI at identical room temperature conditions.

3.4.4. Correlating to Langmuir and Freundlich Isotherms

Analysis of isotherm is considered to be quite significant for quantifying the adsorbent's maximum adsorption capacity and the thermodynamics associated with the phenomenon. Here, I am relating the adsorption isotherm for the prepared material, with the help of Langmuir and Freundlich isotherm models (fig. 14, 15). The equation of Langmuir adsorption isotherm[36] model is,

$$\frac{1}{q_e} = \frac{1}{q_m} + \frac{1}{q_m \times b} \times \frac{1}{C_e}$$

Here, q_e (mg.g^{-1}) described amount of MO adsorbed by the adsorbent (per unit mass), q_m defines maximum adsorption capacity, C_e (mg. L^{-1}) is the amount of dye adsorbed till equilibrium, b (L. mg^{-1}) is the Langmuir constant, and it relates the affinity of binding sites. Separation or equilibrium parameter (R_L) is calculated to find out the isotherm's favorability towards adsorption (favorable ($0<R_L<1$) or not ($R_L > 1$)).[36]

$$R_L = \frac{1}{1 + b \times C_0}$$

Here, C_0 and b represent the initial dye concentration (mg. L^{-1}) and the Langmuir constant (L. mg^{-1}). The Freundlich equation[36] is written as,

$$Ln\ q_e = Ln\ K_f + \frac{1}{n} \times Ln\ C_e$$

Here, q_e and C_e have same meanings, as mentioned earlier in Langmuir isotherm's explanation. K_F (mg. g^{-1}) denotes Freundlich constants and correlates to the adsorption capacity of the material and n is the adsorption strength. In Freundlich isotherm n value reveals whether the adsorption is favorable or not. If the valve of $n<1$, the adsorption is said to be unfavorable and if the value of $n>1$ the adsorption is said to be favourable.

3.4.4.1. For CD/PANI:

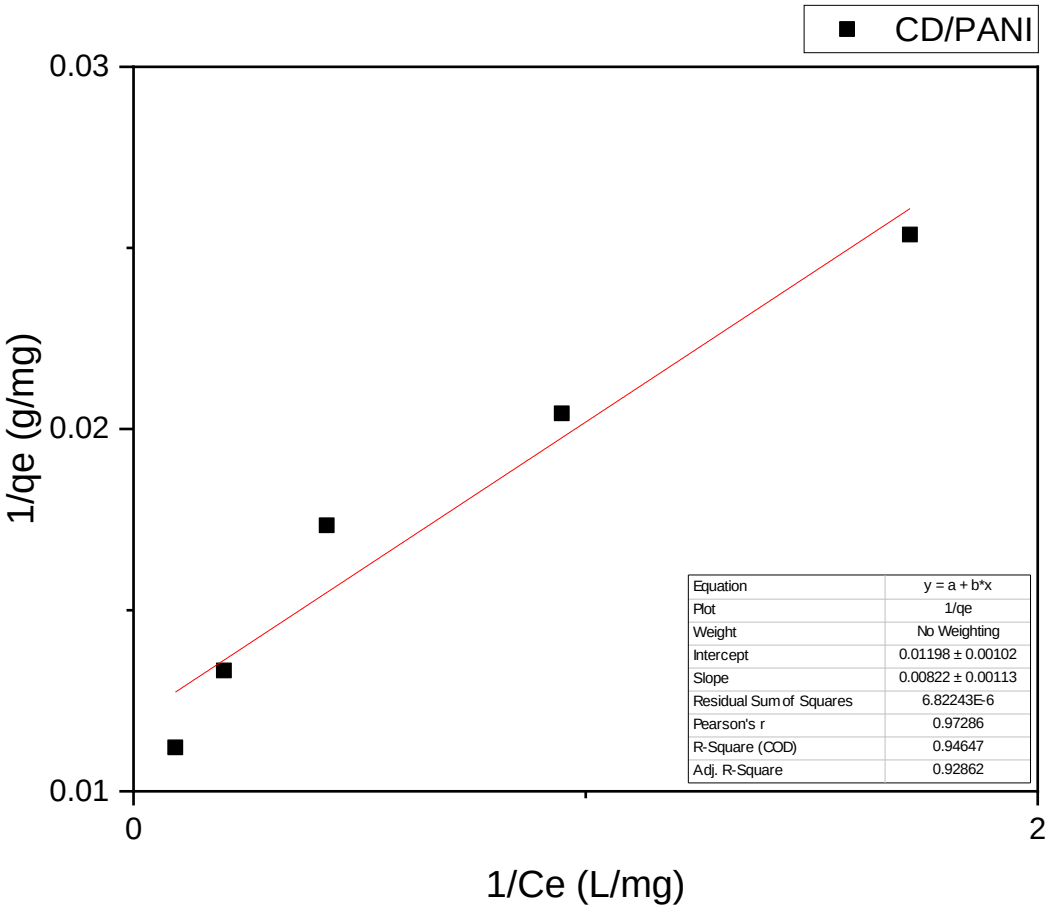

***Figure 15**: Langmuir plot for CD/PANI.*

The values of q_m and b are calculated using the values of slope and intercept values from the above plot, these values and calculations are mentioned below,

$$Slope = 0.00822$$

$$Intercept = 0.01198$$

Using the value of this line's slope K_1 is calculated using equation of pseudo first order rate kinetics as,

$$q_m = \frac{1}{0.01198} = 83.47245\ mg.g^{-1}$$

$$b = \frac{1}{0.00822 \times 83.47245} = 1.45742\ L.mg^{-1}$$

Using the calculated value of b, R_L is calculated which helps us in commenting on the favorability of the adsorption taking place.

$$R_L = \frac{1}{1 + 1.45742 \times 100} = 0.00681$$

As R_L value lies between 0 and 1, the reaction turns out to be favorable.

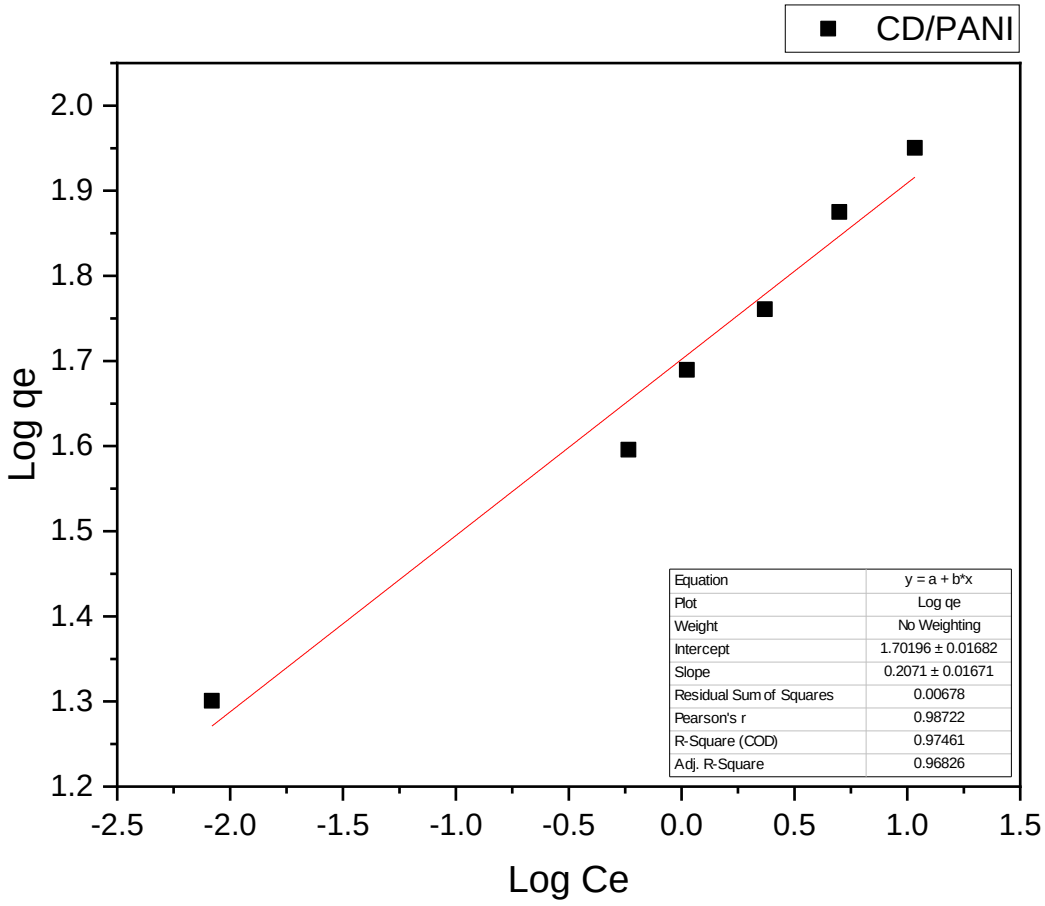

***Figure 16**: Freundlich plot for CD/PANI.*

The values of K_F and n are calculated using the values of slope and intercept values from the above plot, these values and calculations are mentioned below,

$$Slope = 0.2071$$

$$Intercept = 1.70196$$

Using the value of this line's intercept K_F is calculated by correlating to Langmuir's equation,

$$K_F = e^{1.70196} = 5.48469$$

$$n = \frac{1}{0.2071} = 4.82859$$

3.4.4.2. For PANI:

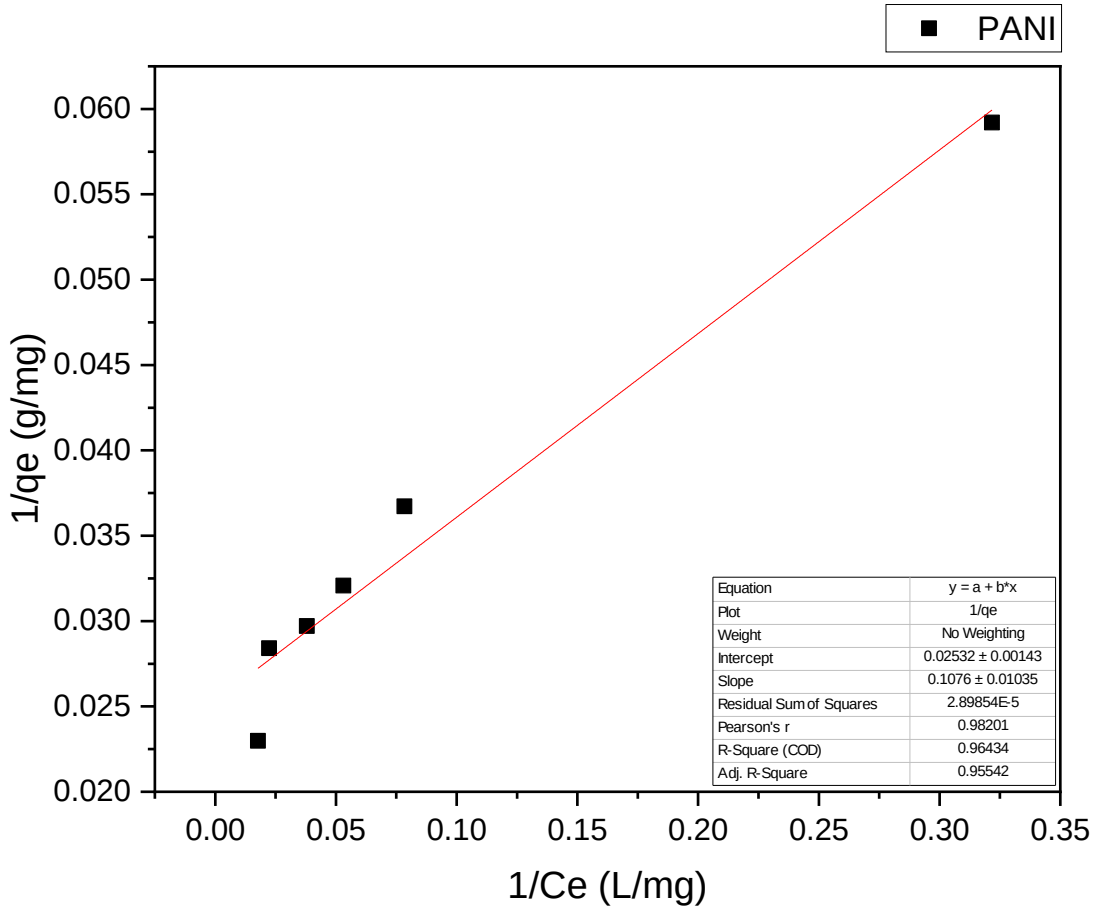

***Figure 17**: Langmuir plot for PANI.*

The values of q_m and b are calculated using the values of slope and intercept values from the above plot, these values and calculations are mentioned below,

$$Slope = 0.1076$$

$$Intercept = 0.02532$$

Using the value of this line's slope K_1 is calculated using equation of pseudo first order rate kinetics as,

$$q_m = \frac{1}{0.02532} = 39.49447\ mg.g^{-1}$$

$$b = \frac{1}{0.1076 \times 39.49447} = 0.23532\ L.mg^{-1}$$

Using the calculated value of b, R_L is calculated which helps us in commenting on the favorability of the adsorption taking place.

$$R_L = \frac{1}{1 + 0.23532 \times 100} = 0.04076$$

As R_L value lies between 0 and 1, the reaction turns out to be favorable.

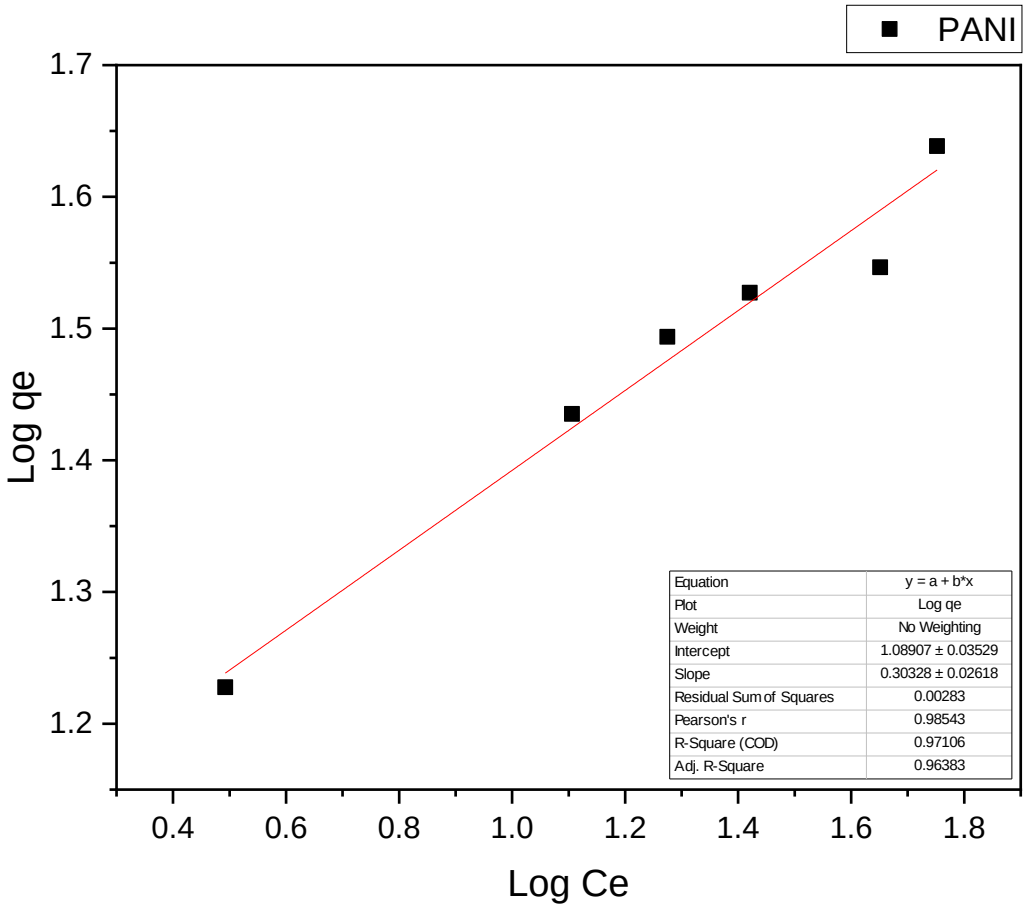

***Figure 18**: Freundlich plot for PANI.*

The values of K_F and n are calculated using the values of slope and intercept values from the above plot, these values and calculations are mentioned below,

$$Slope = 0.30328$$

$$Intercept = 1.08907$$

Using the value of this line's intercept K_F is calculated by correlating to Langmuir's equation,

$$K_F = e^{1.08907} = 2.97151$$

$$n = \frac{1}{0.30328} = 3.29728$$

***Table 5**: Values associated with adsorption isotherms*.

S. No.	Adsorbents	Langmuir				Freundlich		
		R^2	q_m ($mg.g^{-1}$)	b ($L.mg^{-1}$)	R_L	R^2	n	K_F
1.	CD/PANI	0.92862	83.47245	1.45742	0.00681	0.96826	4.82859	5.48469
2.	PANI	0.95542	39.49447	0.23532	0.04076	0.96383	3.29728	2.97151

On the basis of above results from correlations drawn between experimental results and adsorption isotherm equations by Langmuir and Freundlinch, very important understanding is achieved. q_m value signifies the maximum adsorption capacity of the material, it is more than double for CD/PANI as compared to PANI. Also, the value of n was higher than 1 for both the materials, thus theoretically speaking adsorption of MO dye is favorable for both the materials in aqueous conditions.

3.4.5. Maximum Adsorption Capacity of PANI and CD/PANI

Equilibrium concentrations of the resultant solutions are plotted against the respective adsorption capacities, for both the materials. The maximum adsorption capacity of a material is figured out by plotting fitting curves for the values attained in adsorption capacity v/s concentration plots and getting the value at which the curve becomes constant. The adsorption capacity attained by this method is termed to be maximum because as the equilibrium concentration of the remaining dye solution rises, it means that every adsorbent particle is fully loaded with the maximum amount of dye molecules possible.

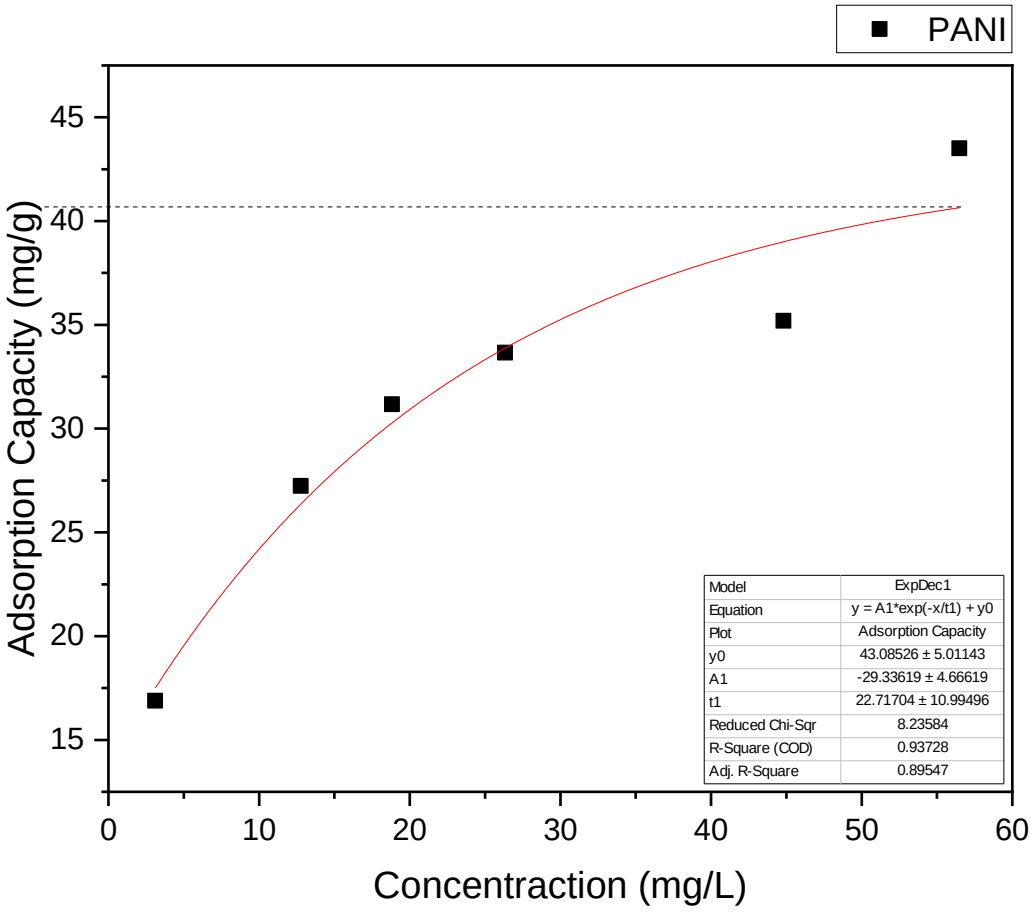

***Figure 19**: Getting the value of maximum adsorption capacity of PANI.*

For PANI, the value of q_{max} came out to be,

$$q_{max} = 40.47\ mg.g^{-1}$$

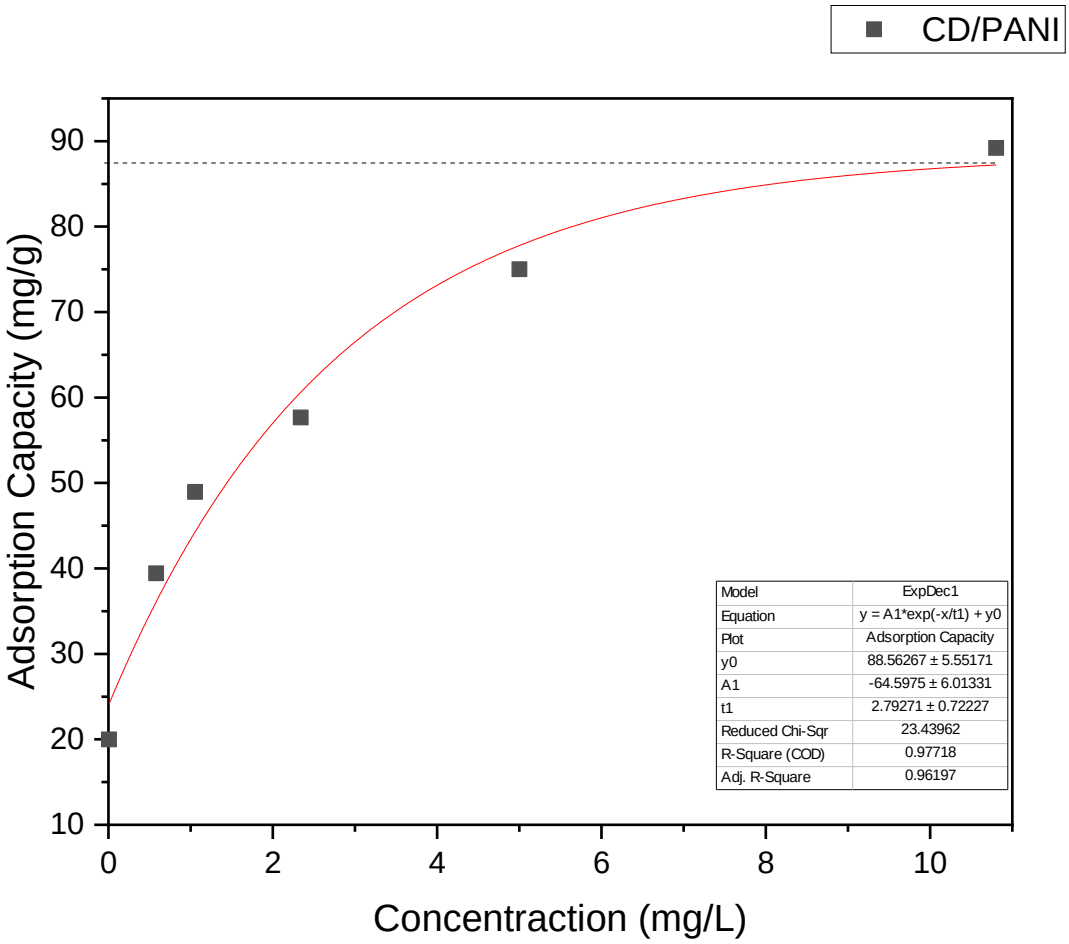

***Figure 20**: Getting the value of maximum adsorption capacity of PANI.*

For CD/PANI, the value of q_{max} is found to be,

$$q_{max} = 87.24\ mg.g^{-1}$$

Thus, the value of maximum adsorption capacity for CD/PANI comes out to be more than double than the value received for PANI. This means that the adsorption sites almost doubled due to the inclusion of CDs into the PANI matrix.

Chapter 4 Conclusions

The desired nanocomposite was successfully prepared and thorough characterizations were done in order to observe the difference in properties between PANI and CD/PANI. All the results point towards successful synthesis of the material. XRD displays the characteristic peaks associated with the matriz material. FTIR plots showed slight difference in the wave number of the peaks, overall general shifting of peaks was observed towards a lower wave number. This is caused because of bond modulations introduced by CD's presence in the matrix. The TGA plots displayed the difference in compositions of the two. Carbon dots are clearly observable on the surface of the polymer in the FESEM images. The polymer is observed to have similar morphology in both of the cases.

The adsorption studies clearly indicate the huge difference in the adsorption capabilities of the two materials. Firstly, higher values of R^2 (the correlation factor) for the for the pseudo-second order kinetics in case of both, PANI and CD/PANI are received. This indicates the nature of adsorption kinetics towards being second order in both the cases. The adsorption capacities (q_e) are almost the same in value for both the adsorbents. The major difference lies in the values of rate constants (K_2) of the two adsorbents. As K_2 value of CD/PANI is more than 20 times that of PANI. Indicating that the rate of adsorption of the same dye being 20 times faster in the presence of CD/PANI than in the presence of same amount of PANI at identical room temperature conditions. This fact alone goes on a huge length to justify the incorporation of CDs onto PANI in a desire for better dye removal properties.

The value for maximum adsorption capacity comes out to be 87.24 $mg.g^{-1}$, while that of pure PANI is only 40.47 $mg.g^{-1}$, despite being prepared under the same conditions.

References

1. Ajekwene, K. K. & Kurian, T. Bulk and nano-structured polyaniline : synthesis , characterization , thermal behaviour and dc conductivity. **6**, (2018).

2. Devadas, B. & Imae, T. Effect of Carbon Dots on Conducting Polymers for Energy Storage Applications. *ACS Sustain. Chem. Eng.* **6**, 127–134 (2018).

3. Mekonnen, M. M. & Hoekstra, A. Y. Global Gray Water Footprint and Water Pollution Levels Related to Anthropogenic Nitrogen Loads to Fresh Water. *Environ. Sci. Technol.* **49**, 12860–12868 (2015).

4. Boënne, W., Desmet, N., Van Looy, S. & Seuntjens, P. Use of online water quality monitoring for assessing the effects of WWTP overflows in rivers. *Environ. Sci. Process. Impacts* **16**, 1510–1518 (2014).

5. Gupta, V. K., Ali, I., Saleh, T. A., Nayak, A. & Agarwal, S. Chemical treatment technologies for waste-water recycling - An overview. *RSC Adv.* **2**, 6380–6388 (2012).

6. Zhao, G. *et al.* Sulfonated graphene for persistent aromatic pollutant management. *Adv. Mater.* **23**, 3959–3963 (2011).

7. Tan, I. A. W., Hameed, B. H. & Ahmad, A. L. Equilibrium and kinetic studies on basic dye adsorption by oil palm fibre activated carbon. *Chem. Eng. J.* **127**, 111–119 (2007).

8. Wong, Y. C., Szeto, Y. S., Cheung, W. H. & McKay, G. Equilibrium studies for acid dye adsorption onto chitosan. *Langmuir* **19**, 7888–7894 (2003).

9. Atchudan, R., Edison, T. N. J. I., Perumal, S., Vinodh, R. & Lee, Y. R. In-situ green synthesis of nitrogen-doped carbon dots for bioimaging and TiO2 nanoparticles@nitrogen-doped carbon composite for photocatalytic degradation of organic pollutants. *J. Alloys Compd.* **766**, 12–24 (2018).

10. Saravanan, R. *et al.* Conducting PANI stimulated ZnO system for visible light photocatalytic degradation of coloured dyes. *J. Mol. Liq.* **221**, 1029–1033 (2016).

11. Zhao, Z. & Xie, Y. Enhanced electrochemical performance of carbon quantum dots-polyaniline hybrid. *J. Power Sources* **337**, 54–64 (2017).

12. Alaş, M. Ö., Güngör, A., Genç, R. & Erdem, E. Feeling the power: robust supercapacitors from nanostructured conductive polymers fostered with Mn 2+ and carbon dots . *Nanoscale* **11**, 12804–12816 (2019).

13. Wang, X., Zhang, J., Zou, W. & Wang, R. Facile synthesis of polyaniline/carbon dot nanocomposites and their application as a fluorescent probe to detect mercury. *RSC Adv.* **5**, 41914–41919 (2015).

14. Pandey, I. & Jha, S. S. Molecularly imprinted polyaniline-ferrocene-sulfonic acid-Carbon dots modified pencil graphite electrodes for chiral selective sensing of D-Ascorbic acid and L-Ascorbic acid: A clinical biomarker for preeclampsia. *Electrochim. Acta* **182**, 917–928 (2015).

15. Elnaggar, E. M., Kabel, K. I., Farag, A. A. & Al-Gamal, A. G. Comparative study on doping of polyaniline with graphene and multi-walled carbon nanotubes. *J. Nanostructure Chem.* **7**, 75–83 (2017).

16. Xu, X. *et al.* Electrophoretic analysis and purification of fluorescent single-walled carbon nanotube fragments. *J. Am. Chem. Soc.* **126**, 12736–12737 (2004).

17. Hsu, P. C., Shih, Z. Y., Lee, C. H. & Chang, H. T. Synthesis and analytical applications of photoluminescent carbon nanodots. *Green Chem.* **14**, 917–920 (2012).

18. Li, H., Kang, Z., Liu, Y. & Lee, S. T. Carbon nanodots: Synthesis, properties and applications. *J. Mater. Chem.* **22**, 24230–24253 (2012).

19. Chen, F. & Liu, P. Conducting polyaniline nanoparticles and their dispersion for waterborne corrosion protection coatings. *ACS Appl. Mater. Interfaces* **3**, 2694–2702 (2011).

20. Amado, F. D. R. *et al.* High-impact polystyrene/polyaniline membranes for acid solution treatment by electrodialysis: Preparation, evaluation, and chemical calculation. *J. Colloid Interface Sci.* **320**, 52–61 (2008).

21. Qiao, Y. *et al.* Nanostructured Polyaniline / Titanium Fuel Cells. *ACS Nano* **2**, 113–119 (2008).

22. Alam, J., Dass, L. A., Alhoshan, M. S., Ghasemi, M. & Mohammad, A. W. Development of polyaniline-modified polysulfone nanocomposite membrane. *Appl. Water Sci.* **2**, 37–46 (2012).

23. Liu, J. *et al.* Room-temperature magnetism in carbon dots and enhanced ferromagnetism in carbon dots-polyaniline nanocomposite. *Sci. Rep.* **7**, 1–7 (2017).

24. Ganguly, S., Das, P., Banerjee, S. & Das, N. C. Advancement in science and technology of carbon dot-polymer hybrid composites: a review. *Funct. Compos. Struct.* **1**, 022001 (2019).

25. Ameen, S., Im, Y. Bin, Jo, C. G., Kim, Y. S. & Shin, H. S. Synthesis and characterization of polyaniline/MCM-41 nanocomposites and their photocatalytic activity. *J. Nanosci. Nanotechnol.* **11**, 541–545 (2011).

26. Zhang, S. *et al.* Hierarchical nanocomposites of polyaniline nanorods arrays on graphitic carbon nitride sheets with synergistic effect for photocatalysis. *Catal. Today* **224**, 114–121 (2014).

27. Ayad, M., El-Hefnawy, G. & Zaghlol, S. Facile synthesis of polyaniline nanoparticles; its adsorption behavior. *Chem. Eng. J.* **217**, 460–465 (2013).

28. Ayad, M. M. & El-Nasr, A. A. Adsorption of cationic dye (methylene blue) from water using polyaniline nanotubes base. *J. Phys. Chem. C* **114**, 14377–14383 (2010).

29. Ayad, M. M., Abu El-Nasr, A. & Stejskal, J. Kinetics and isotherm studies of methylene blue adsorption onto polyaniline nanotubes base/silica composite. *J. Ind. Eng. Chem.* **18**, 1964–1969 (2012).

30. Ayad, M. & Zaghlol, S. Nanostructured crosslinked polyaniline with high surface area: Synthesis, characterization and adsorption for organic dye. *Chem. Eng. J.* **204**–

205, 79–86 (2012).

31. Tanzifi, M. *et al.* Artificial neural network optimization for methyl orange adsorption onto polyaniline nano-adsorbent: Kinetic, isotherm and thermodynamic studies. *J. Mol. Liq.* **244**, 189–200 (2017).

32. Xia, Y., Li, T., Chen, J. & Cai, C. Polyaniline (skin)/polyamide 6 (core) composite fiber: Preparation, characterization and application as a dye adsorbent. *Synth. Met.* **175**, 163–169 (2013).

33. De, B. & Karak, N. A green and facile approach for the synthesis of water soluble fluorescent carbon dots from banana juice. *RSC Adv.* **3**, 8286–8290 (2013).

34. Konyushenko, E. N. *et al.* Polyaniline nanotubes: Conditions of formation. *Polym. Int.* **55**, 31–39 (2006).

35. Ho, Y. . & McKay, G. Pseudo-second order model for sorption processes. *Process Biochem.* **34**, 451–465 (1999).

36. LeVan, M. D. & Vermeulen, T. Binary Langmuir and Freundlich isotherms for ideal adsorbed solutions. *J. Phys. Chem.* **85**, 3247–3250 (1981).